Instanton calculus in shell models of turbulence

Isabelle Daumont,[1,2] Thierry Dombre,[1] and Jean-Louis Gilson[1]

[1]*Centre de Recherches sur les Très Basses Températures-CNRS, Laboratoire Conventionné Avec l'Université Joseph Fourier,
Boîte Postale 166, 38042 Grenoble Cédex 9, France*

[2]*Ecole Normale Supérieure de Lyon, Laboratoire de Physique, 46 Allée d'Italie, 69364 Lyon Cédex 07, France*

It has been shown recently that the intermittency of the Gledzer-Ohkitani-Yamada (GOY) shell model of turbulence has to be related to singular structures whose dynamics in the inertial range includes interactions with a background of fluctuations. In this paper we propose a statistical theory of these objects by modeling the incoherent background as a Gaussian white-noise forcing of small strength Γ. A general scheme is developed for constructing instantons in spatially discrete dynamical systems and the Cramér function governing the probability distribution of effective singularities of exponent z is computed up to first order in a semiclassical expansion in powers of Γ. The resulting predictions are compared with the statistics of coherent structures deduced from full simulations of the GOY model at very high Reynolds numbers.

I. INTRODUCTION

Are structures (sheets or filaments of vorticity) a vital ingredient of intermittency in three-dimensional (3D) incompressible turbulence? To date, this important question remains open [1], and an answer starting from first principle, i.e., from a controlled approximation to the Navier-Stokes equations, seems over the horizon. The new understanding of the anomalous scaling in the Kraichnan's model of passive advection [2], based on the identification of zero modes in the homogeneous Hopf equations for equal-time correlators, has in particular strengthened the belief that field-theoretical methods would eventually be able to capture the full statistics of turbulent flows without an explicit account of structures.

Interestingly enough, the relative interplay between coherent ordered structures and incoherent turbulent fluctuations turns out to be a subtle matter already in the restricted framework of the so-called shell models of turbulence [3]. It was noticed very soon [4] that elementary bricks of intermittency in those deterministic one-dimensional (1D) cascade models could be pulses or bursts of activity growing in an almost self-similar way as they move from large to small scales. However, genuine dynamically stable self-similar solutions of the equations of motion in the inertial range display a unique scaling exponent (to be denoted below as z_0), provided they are localized in **k** space (which, in the shell model approach, reduces to a discrete set of wave numbers $k_n = 2^{(n-1)}$, where the shell index n goes from 1 to ∞). Furthermore, the exponent z_0, giving the logarithmic slope of the velocity gradient spectrum left in the trail of the pulse, happens to be rather close to the Kolmogorov value 2/3 ($z_0 = 0.72$) in the case of the Gledzer-Ohkitani-Yamada (GOY) model, in the range of parameters where it reproduces at best the multiscaling properties of real turbulent flows.

In Ref. [5] the role played by the interaction of pulses with the rest of the flow in producing more singular events was unraveled, and a two-fluid picture was introduced, where coherent structures form in and propagate into a featureless random background. Our goal in this paper is to elevate this still rather qualitative proposal to the rank of a semiquantitative theory and to test its predictive power about intermittency in the GOY model. We shall assume that turbulent fluctuations on the shells downstream of the pulse, i.e., small scales, act on the coherent part of the flow as a random, white-in-time, Gaussian forcing and we ask whether the inviscid stochastic extension of the GOY model obtained in this way is able to reproduce the statistics of strong deviations of the full turbulent system in the inertial range. There is *a priori* quite a lot of freedom in the parametrization of the forcing. Therefore, in order to keep things as simple as possible, we bind ourselves to use a single adjustable parameter (hereafter noted Γ), which measures the level of noise. We consider the semiclassical limit $\Gamma \ll 1$ of these systems and study the statistics of singular structures appearing in this regime [6].

Semiclassical (or instanton) techniques are well suited to capture large and rare excursions of fluctuating fields [7]. As such, they have gained recently a renewal of interest in the field of turbulence [8] and have already led to noteworthy results in the context of Burger's turbulence [9,10], and of the Kraichnan's model of passive scalar advection [11,12]. One usually starts from a path-integral representation of high-order structure functions and uses a saddle-point approximation to determine the coupled field-force configurations contributing mostly to those quantities. The nature of the statistical object to be computed imposes precise boundary conditions on the physical field and the random force (respectively at large and small scales, where the cascade processes start and end). Instantons, which in the inertial range often reduce to a self-similar collapse along some spatial dimensions, are eventually selected by a delicate matching procedure at the two boundaries. In shell models we are dealing with an intrinsically discrete lattice of logarithmic scales. As a consequence, the analytic computation of instantons is completely out of reach in the inertial range, not to mention the matching on both sides of the cascade. To circumvent this difficulty, we shall focus on the probability distribution function (pdf) of scaling exponents after n cascade steps, $P_n(z)$, and argue that, in the semiclassical limit

$\Gamma \ll 1$, this pdf builds up from the neighborhood of a single self-similar instanton (of scaling exponent z) that dynamic stability considerations will help us to construct numerically. In order to get nontrivial physics, it turns out to be necessary to perform the semiclassical expansion of $-\lim_{n\to\infty}(1/n)\ln P_n(z)$ (the rate of rarefaction of singularities of the scaling exponent z in the multifractal picture) up to next to leading order in powers of Γ. This can be achieved via a summation over quadratic fluctuations around the instantons, once the proper set of boundary conditions for the corresponding trajectories in configuration space has been defined. We shall show in detail how to carry out this program and end up with a prediction for $P_n(z)$ lending itself to a straight confrontation with the pdf of effective scaling exponents of coherents events that can be extracted from simulations of the GOY model at very high Reynolds numbers. Although our interest lies primarily in gaining a better understanding of intermittency in the framework of shell models of turbulence, the emphasis will be put in this paper on the technical aspects of the method that we had to develop for computing instantons. We believe that this method is general enough to find applications in other contexts or physical problems, like for instance the motion of complex objects or excitations on one-dimensional (1D) lattices in the presence of a comoving random environment.

The paper is organized as follows. In Sec. II we define the stochastic extensions of the GOY model that we shall study. In Sec. III the equations of motion for instantons will be derived using the well-known Martin-Siggia-Rose path-integral representation of probability distribution functions for stochastic dynamical systems. Section IV is devoted to the computation of self-similar extremal trajectories, with the theoretical considerations underlying the solution explained in Sec. IV A and its practical implementing, together with the results, exposed in Sec. IV B. The important effect of quadratic fluctuations and the rather heavy formal work behind their computation are discussed in Sec. V. The comparison of the results issuing from the instanton approach with numerical data on the statistics of coherent structures in the genuine GOY model is given in Sec. VI. We conclude in Sec. VII, in particular as to the relevance of a two-fluid description of intermittency in shell models of turbulence.

II. DEFINITION OF THE STOCHASTIC DYNAMICAL SYSTEM

Equations of motion for the GOY model in the inertial range read

$$\frac{db_n}{dt} = Q^2(1-\epsilon)b_{n-2}^* b_{n-1}^* + \epsilon b_{n-1}^* b_{n+1}^* - Q^{-2}b_{n+1}^* b_{n+2}^*,$$
$$(2.1)$$

where the complex variable $b_n = k_n u_n$ should be understood as the Fourier component of the gradient velocity field at wave number $k_n = Q^n$ and the integer n runs from 0 to $+\infty$. Throughout this paper, usual values of parameters $\epsilon = 0.5$ and $Q = 2$ will be assumed. It is convenient to cast Eq. (2.1) in a vectorial form

$$\frac{d\mathbf{b}}{dt} = \mathbf{N}[\mathbf{b}], \qquad (2.2)$$

where the infinite-dimensional vector $\mathbf{b}$ is built up from the b_n's, while the nth component of the nonlinear kernel $\mathbf{N}[\mathbf{b}]$ is given by the right-hand side of Eq. (2.1). It is worth noting at this point that $\mathbf{b}^* \cdot \mathbf{b} = \Sigma_{n=0}^{\infty} |b_n|^2$ plays dimensionally the role of enstrophy in real flow and that the inverse square root of this quantity sets the order of magnitude of the smallest time scale on the shell lattice.

Since quadratic nonlinearities lead generically to finite time singularities, it is very useful to introduce a desingularizing time variable τ related to the physical time t by the differential law

$$\frac{d\tau}{dt} = (\mathbf{b}^* \cdot \mathbf{b})^{1/2}. \qquad (2.3)$$

This turns Eq. (2.2) into

$$\frac{d\mathbf{b}}{d\tau} = \frac{\mathbf{N}[\mathbf{b}]}{(\mathbf{b}^* \cdot \mathbf{b})^{1/2}}, \qquad (2.4)$$

where both sides of the equation have the same scaling dimension in the field $\mathbf{b}$, which shows that an infinite ''time'' is now required to form a singularity by traveling across the whole shell axis.

From previous work [13], we know that every initial condition of finite enstrophy, when evolving under dynamics (2.4), eventually organizes itself in a solitonlike pulse, moving from large to small scales at a constant speed with an exponential growth of its amplitude. The asymptotic state is unique, up to trivial phase symmetries of the GOY model [14], time translations, or multiplicative rescaling of the field $\mathbf{b}$, which all leave the equation of motion (2.4) invariant. We may restrict our attention without loss of generality to the case where the phase pattern along the shell axis does not break into a three-sublattice structure. The asymptotic Floquet state, to be noted henceforth $\mathbf{b}^0(\tau)$, is then purely real and such that

$$b_{n+1}^0(\tau + T_0) = \exp(A_0 T_0) b_n^0(\tau). \qquad (2.5)$$

The period T_0 is the ''time'' needed for the center of the pulse to go from shell n to shell $n+1$, while the (positive) Lyapunov exponent A_0 controls its growth. Both quantities T_0 and A_0, are dynamically selected in a unique way. The scaling exponent z_0 associated with the pulse (fixing in particular the logarithmic slope of the spectrum left in its trail) can be extracted from the identity $Q^{z_0} = \exp(A_0 T_0)$. Its value turns out to be 0.72 in the case of the GOY model for the choice of parameters stated before.

We turn now to the stochastic models that we are interested in solving by the instanton method. Their physical motivation has been explained in Ref. [5]: we assume that pulses parametrize adequately singular (and temporally coherent) structures in shell models but that the deterministic dynamics (2.2) should be enlarged towards a stochastic one, in order to describe the interaction of a given pulse with incoherent fluctuations produced by the relaxation of the

trails left by its predecessors. We are therefore led to consider the following extension of the original inviscid GOY model:

$$\frac{d\mathbf{b}}{dt} = \mathbf{N}[\mathbf{b}] + \sqrt{\Gamma}(\mathbf{b}^* \cdot \mathbf{b})^{3/4} B[\mathbf{C}] \boldsymbol{\eta}, \qquad (2.6)$$

where $\boldsymbol{\eta}$ is a Gaussian noise, δ-correlated in time and shell index, whose correlations read

$$\langle \eta_n^*(t) \eta_{n'}(t') \rangle = \delta_{nn'} \delta(t-t'). \qquad (2.7)$$

The various factors coming in front of $\boldsymbol{\eta}$ in Eq. (2.6) have the following meaning: the number Γ fixes the relative strength of incoherent fluctuations with respect to coherent ones and we shall be interested in the semiclassical limit of small Γ amenable to semianalytic treatment. As will be clearer in a while, the overall scale factor $(\mathbf{b}^* \cdot \mathbf{b})^{3/4}$ is there to keep noise relevant all along the cascade, thereby preserving scale invariance. Finally the matrix $B[\mathbf{C}]$, of zero scaling dimension in the field $\mathbf{b}$ since it depends only on the unit vector $\mathbf{C} = \mathbf{b}/\sqrt{(\mathbf{b}^* \cdot \mathbf{b})}$, may be used either to introduce spatial correlations of noise (along the shell axis) or to localize its action with respect to the instantaneous position of the pulse. Although the formalism to be developed in this paper can deal with the most general situation, we restricted ourselves in practical investigations to diagonal matrices $B[\mathbf{C}]$, just playing with the degree of localization of noise. Results will be presented for three rather emblematic choices of B: (i) $B_{nn} = 1$, which describes a completely delocalized noise; (ii) $B_{nn} = C_{n-2}^* C_{n-1}^*$, which keeps some flavor of the original GOY dynamics and makes noise active just at the leading edge of the pulse; and finally (iii) $B_{nn} = |C_{n-5}|^2 + |C_{n-4}|^2$, which removes the action of noise further away from the center of the pulse. We must emphasize that these particular choices were not dictated by rigorous considerations on the underlying dynamics of the GOY model, but rather used to scan the variety of behaviors which may be expected from such stochastic dynamical systems. It should be noted that the structure of the matrix B is not constrained by any conservation law, since the coherent part of the flow does not form a closed system anymore, even in the inertial range, in our two-fluid description. Finally, to simplify the following analysis, we are going to restrict the fields $\mathbf{b}$ and $\boldsymbol{\eta}$ in Eqs. (2.6) and (2.7) to being real-valued vectors and to neglect the effect of imaginary fluctuations. This is certainly not a serious restriction as for the instantons themselves, which are expected to be, like the self-similar deterministic solution described above, purely real, up to trivial phase symmetries of the GOY model. It can also be remarked that the model (ii) (which will be found later on to give the more convincing results) does not require a complex noise, since the phase degrees of freedom have already been incorporated in the definition of the matrix B in that case.

While the deterministic dynamics (2.2) selects a single self-similar solution exploding in finite time with scaling exponent z_0, the presence of noise in Eq. (2.6) allows for a continuum of scaling exponents, even in the manifold of normalizable fields $\mathbf{b}$. In the small noise (or semiclassical) limit

$\Gamma \ll 1$, the probability density of developing an effective growth exponent z after $n \gg 1$ cascade steps will take the form

$$P_n(z) \sim \sqrt{n} \exp\left[-n\left(\frac{s_0(z)}{\Gamma} + s_1(z) \right) \right], \qquad (2.8)$$

where $s_0(z)$ is the action per unit cascade step of the self-similar extremalsolution of scaling exponent z of optimal bare Gaussian weight (or instanton), and $s_1(z)$ measures, to the lowest order in Γ, how the basin of attraction of the instanton in phase space evolves with the number of cascade steps. Note that the argument of the exponential in Eq. (2.8), $-\{[s_0(z)/\Gamma] + s_1(z)\}$, is nothing but the Cramér function introduced in the theory of large deviations, which governs the rate of rarefaction of singularities in the multifractal picture [15]. We will show in this paper how to compute in a clean way both quantities $s_0(z)$ and $s_1(z)$. Before doing this, we must carefully handle problems related to the time discretization of the stochastic equation (2.6) since a consistent treatment of them is necessary to get the right expression of the first correction $s_1(z)$. We shall adopt the view that the initial stochastic equation (2.6) is to be understood in the Stratonovich sense [16]. However, in the path-integral formulation of stochastic dynamical systems that we shall heavily use in the following, it is much simpler to work with the Ito prescription which, in the limit of small time steps, amounts integrating Eq. (2.6) within a basic Euler scheme with all $\mathbf{b}$-dependent quantities in the right-hand side (rhs) estimated at the prepoint. When switching to the Ito discretization recipe, the stochastic equation has to be changed into

$$\frac{d\mathbf{b}}{dt} = \mathbf{N}_\Gamma[\mathbf{b}] + \sqrt{\Gamma}(\mathbf{b} \cdot \mathbf{b})^{3/4} B[\mathbf{C}] \boldsymbol{\eta}, \qquad (2.9)$$

where the new kernel $\mathbf{N}_\Gamma[\mathbf{b}]$ differs from $\mathbf{N}[\mathbf{b}]$ by the addition of the so-called Ito drift term. We give, for the sake of completeness, the resulting expression of the nth component of $\mathbf{N}_\Gamma$,

$$N_{\Gamma\,n}[\mathbf{b}] = N_n[\mathbf{b}] + \frac{1}{2}\Gamma\frac{\partial}{\partial b_k}[(\mathbf{b} \cdot \mathbf{b})^{3/4} B_{nj}](\mathbf{b} \cdot \mathbf{b})^{3/4} B_{kj}. \quad (2.10)$$

At this point, we may write down the discrete analog of Eq. (2.3) as $\Delta\tau_i = \tau_{i+1} - \tau_i = (\mathbf{b}_i \cdot \mathbf{b}_i)^{1/2}(t_{i+1} - t_i)$ (where i is the time index) and redefine the noise as $\boldsymbol{\eta}_i \to \boldsymbol{\xi}_i = \sqrt{\Gamma}(\mathbf{b}_i \cdot \mathbf{b}_i)^{-1/4}\boldsymbol{\eta}_i$. This leads to the following stochastic extension of Eq. (2.4) which will be the starting point of our formal analysis,

$$\frac{d\mathbf{b}}{d\tau} = \frac{\mathbf{N}_\Gamma[\mathbf{b}]}{(\mathbf{b} \cdot \mathbf{b})^{1/2}} + (\mathbf{b} \cdot \mathbf{b})^{1/2} B[\mathbf{C}] \boldsymbol{\xi}, \qquad (2.11)$$

with

$$\langle \xi_n(\tau) \xi_{n'}(\tau') \rangle = \Gamma \delta_{nn'} \delta(\tau-\tau'). \qquad (2.12)$$

III. EXTREMAL TRAJECTORIES FROM PATH-INTEGRAL FORMULATION

Statistics of classical fields in the presence of random forces can be examined with the help of field theoretical techniques formulated in [17]. In particular, the probability to go from point $\mathbf{b}_{in}$ at time $\tau = 0$ to point $\mathbf{b}_f$ at time τ_f may be written as a path integral

$$P(\mathbf{b}_{in},0;\mathbf{b}_f,\tau_f) = \int \mathcal{D}\mathbf{b}\mathcal{D}\mathbf{p}\exp - S[\mathbf{b},\mathbf{p}], \qquad (3.1)$$

where $S[\mathbf{b},\mathbf{p}]$ is an effective action to be defined below, $\mathbf{p}$ an auxiliary field conjugated to the physical one $\mathbf{b}$ and $\mathcal{D}\mathbf{b}\mathcal{D}\mathbf{p}$ stands for

$$\frac{d\mathbf{p}_0}{(2\pi)^d} \prod_{i=1}^{i=N-1} \frac{d\mathbf{b}_i d\mathbf{p}_i}{(2\pi)^d}. \qquad (3.2)$$

In the last equation, the time interval τ_f was divided into N subintervals of length $\Delta\tau = \tau_f/N$ (with $\mathbf{b}_{in} = \mathbf{b}_0$ and $\mathbf{b}_f = \mathbf{b}_N$) and the number of shells was set to a finite value d, in order to give a clear meaning to the measure. For the problem of interest (2.11), the effective action S takes the form

$$S[\mathbf{b},\mathbf{p}] = \sum_{i=0}^{i=N-1} i\mathbf{p}_i \cdot \left(\mathbf{b}_{i+1} - \mathbf{b}_i - \Delta\tau \frac{\mathbf{N}_\Gamma[\mathbf{b}_i]}{(\mathbf{b}_i \cdot \mathbf{b}_i)^{1/2}} \right)$$
$$+ \frac{\Gamma}{2}(\mathbf{b}_i \cdot \mathbf{b}_i)\mathbf{p}_i \cdot B[\mathbf{b}_i]^t B[\mathbf{b}_i]\mathbf{p}_i, \qquad (3.3)$$

or, in the continuum limit

$$S[\mathbf{b},\mathbf{p}] = \int_0^{\tau_f} d\tau i\mathbf{p}.\left(\frac{d\mathbf{b}}{d\tau} - \frac{\mathbf{N}_\Gamma[\mathbf{b}]}{(\mathbf{b}\cdot\mathbf{b})^{1/2}} \right)$$
$$+ \frac{\Gamma}{2}(\mathbf{b}\cdot\mathbf{b})\mathbf{p}\cdot B[\mathbf{b}]^t B[\mathbf{b}]\mathbf{p}. \qquad (3.4)$$

The last term in Eq. (3.4), quadratic in $\mathbf{p}$, appears as a result of averaging over the Gaussian noise $\boldsymbol{\xi}$, while the first one, linear in $\mathbf{p}$, would still be there in the absence of noise as a formal way of enforcing the deterministic equation of motion of $\mathbf{b}$. $S[\mathbf{b},\mathbf{p}]$ will be referred to in the following as the Martin-Siggia-Rose (MSR) action.

Rescaling the auxiliary field $\mathbf{p}$ as $\mathbf{p}'/\Gamma$ puts an overall large factor $1/\Gamma$ in front of the effective action and opens the way to a saddle-point approximation to the path integral (3.1). Extremization of the action with respect to the configurations of both fields $\mathbf{b}$ and $\mathbf{p}$ between times 0 and τ_f, for fixed endpoints, leads in a straightforward way to the following set of coupled equations defining extremal trajectories:

$$\frac{d\mathbf{b}}{d\tau} = \frac{\mathbf{N}_\Gamma[\mathbf{b}]}{(\mathbf{b}\cdot\mathbf{b})^{1/2}} + (\mathbf{b}\cdot\mathbf{b})B^t B\boldsymbol{\theta}, \qquad (3.5)$$

$$\frac{d\boldsymbol{\theta}}{d\tau} = -{}^t\mathcal{M}\boldsymbol{\theta} - \frac{1}{2}\partial_\mathbf{b}[(\mathbf{b}\cdot\mathbf{b})\boldsymbol{\theta}\cdot B^t B\boldsymbol{\theta}]. \qquad (3.6)$$

In the above equation, we set $\mathbf{p}' = -i\boldsymbol{\theta}$ and $\mathcal{M}$ is the Jacobian matrix of the kernel $\mathbf{N}_\Gamma[\mathbf{b}]/(\mathbf{b}\cdot\mathbf{b})^{1/2}$:

$$\mathcal{M} = \frac{\partial_\mathbf{b}\mathbf{N}_\Gamma[\mathbf{b}]}{(\mathbf{b}\cdot\mathbf{b})^{1/2}} - \frac{\mathbf{N}_\Gamma[\mathbf{b}]\otimes\mathbf{b}}{(\mathbf{b}\cdot\mathbf{b})^{3/2}}.$$

As usual, Eqs. (3.5) and (3.6) inherit a canonical structure

$$\frac{d\mathbf{b}}{d\tau} = \frac{\partial\mathcal{H}}{\partial\boldsymbol{\theta}}, \qquad (3.7)$$

$$\frac{d\boldsymbol{\theta}}{d\tau} = -\frac{\partial\mathcal{H}}{\partial\mathbf{b}}, \qquad (3.8)$$

where the Hamiltonian $\mathcal{H}$ reads

$$\mathcal{H} = \frac{\boldsymbol{\theta}\cdot\mathbf{N}_\Gamma[\mathbf{b}]}{(\mathbf{b}\cdot\mathbf{b})^{1/2}} + \frac{1}{2}(\mathbf{b}\cdot\mathbf{b})(\boldsymbol{\theta}\cdot B^t B\boldsymbol{\theta}). \qquad (3.9)$$

Since $\mathcal{H}$ is not explicitly time dependent, we conclude that its value, to be called the pseudoenergy in the sequel, is conserved along any extremal trajectory. The action $S[\mathbf{b},\boldsymbol{\theta}]$ may be rewritten in terms of $\mathcal{H}$ as

$$S[\mathbf{b},\boldsymbol{\theta}] = \int_0^{\tau_f} d\tau\left(\boldsymbol{\theta}\cdot\frac{d\mathbf{b}}{d\tau} - \mathcal{H} \right), \qquad (3.10)$$

from which it is seen that the further requirement that the trajectory be extremal with respect to time reparametrization leads to the condition of vanishing pseudoenergy $\mathcal{H} = 0$. Noting that each term of $\mathcal{H}$ in Eq. (3.9) has the same scaling dimension in $\mathbf{b}$ and $\boldsymbol{\theta}$ (either 1 or 2), one finds that

$$\frac{d}{d\tau}(\mathbf{b}\cdot\boldsymbol{\theta}) = \boldsymbol{\theta}\cdot\frac{\partial\mathcal{H}}{\partial\boldsymbol{\theta}} - \mathbf{b}\cdot\frac{\partial\mathcal{H}}{\partial\mathbf{b}} = 0, \qquad (3.11)$$

which shows that the overlap $\mathbf{b}\cdot\boldsymbol{\theta}$ between the physical and auxiliary fields is also conserved, together with $\mathcal{H}$, along an extremal trajectory. This property reflects the scaling invariance of the stochastic cascade processes we have in mind. We should at this point insist on the fact that, in contrast to instantons in the framework of equilibrium statistical mechanics or quantum mechanics, equations for extremal trajectories in stochastic dynamical systems describe the real motion of the physical field in a particular "optimal" realization of the noise. The comparison of Eqs. (2.11) and (3.5) shows indeed that the following relation holds between $\boldsymbol{\xi}$ and $\boldsymbol{\theta}$:

$$\boldsymbol{\xi} = (\mathbf{b}\cdot\mathbf{b})^{1/2}\,{}^t B\boldsymbol{\theta}. \qquad (3.12)$$

Like their deterministic parent (2.4), the equations of motion (3.5) and (3.6) sustain formally traveling-wave-like solutions, such that

$$b_{n+1}(\tau+T) = \exp AT b_n(\tau), \qquad (3.13)$$

$$\theta_{n+1}(\tau+T) = \exp -AT \theta_n(\tau), \qquad (3.14)$$

whose scaling exponent $z = AT/\ln Q$ is expected to be now related to the overlap $\mu_1 = \mathbf{b}\cdot\boldsymbol{\theta}$ (with $z = z_0$ for $\mu_1 = 0$, in the absence of noise). However, there is little hope of finding these solutions by a direct forward in time integration of Eqs. (3.5) and (3.6), as could be done successfully for Eq (2.4).

This is because the auxiliary field $\boldsymbol{\theta}$ intrinsically propagates ''backward'' in time, as is clear from the discretized version of Eq. (3.6) [deduced from the extremization of Eq. (3.3)]. In the present problem, we have observed numerically that regular Floquet states emerge as dynamical attractors of Eqs. (3.5) and (3.6) only for rather high values of μ_1 (otherwise the system evolves in a chaotic manner). They form a branch of solutions definitely distinct from the one to be obtained in the next section and correspond presumably to local maxima of the action rather than the local minima of interest to us.

IV. AN ITERATIVE METHOD FOR COMPUTING SELF-SIMILAR INSTANTONS

A. Theory

The previous considerations suggest that Eqs. (3.5) and (3.6) should not be treated on the same footing. The careful examination of physical properties that instantons should possess will give us keys for computing them. Assume for a while that a solution has been found, obeying Eqs. (3.13) and (3.14). We note the corresponding configurations of $\mathbf{b}$ and $\boldsymbol{\xi}$ as $\mathbf{b}^0$ and $\boldsymbol{\xi}^0$. The linearization of the equation of motion (3.5) at fixed noise leads to the following evolution of fluctuations $\delta\mathbf{b}$ of $\mathbf{b}$ around $\mathbf{b}^0$:

$$\frac{d}{d\tau}\delta\mathbf{b} = \mathcal{L}\delta b = \mathcal{M}\delta\mathbf{b} + (\delta\mathbf{b}\cdot\partial_\mathbf{b})[(\mathbf{b}\cdot\mathbf{b})^{1/2}B\boldsymbol{\xi}^0]|_{b^0}. \quad (4.1)$$

The periodicity properties of the linear operator $\mathcal{L}$ ensure that the fluctuations of $\mathbf{b}$ may be decomposed on a complete set of eigendirections $\boldsymbol{\Psi}_{ir}(\tau)$ evolving according to Eq. (4.1) and such that

$$\boldsymbol{\Psi}_{ir}(\tau+T) = e^{\sigma_i T}\mathcal{T}_{+1}\boldsymbol{\Psi}_{ir}(\tau), \quad (4.2)$$

where $\mathcal{T}_{+1}$ denotes translation by one unit in the right direction along the shell lattice. In practice we shall have to work with a finite number of shells d and, in order to get rid of boundary effects, it will be necessary to fully periodize the shell lattice: the index i then runs between 1 and d and the translation operator is easy to represent as a matrix. Formally, the $\boldsymbol{\Psi}_{ir}$'s can be determined at time $\tau=0$ by diagonalizing the Floquet operator:

$$U_T = \mathcal{T}_{-1}\overleftarrow{\exp}\int_0^T \mathcal{L}d\tau, \quad (4.3)$$

where $\overleftarrow{\exp}$ is a chronologically time-ordered product (initial time on the right). One observes that $\mathbf{b}^0$ satisfies Eq. (4.2) with a time-averaged Lyapunov exponent $\sigma=A$.

We claim now that every initial condition $\mathbf{b}(0)$ evolving in the configuration of noise $\boldsymbol{\xi}_0$ should be attracted towards the instantonic trajectory. If it were not true, some perturbations would be able to grow in the comoving frame of the pulse, thereby generating scaling exponents larger than z at no cost in the action, in contradiction with the hypothesis that the optimal realization of a singularity of exponent z has been found. This strong criterion of dynamic stability is another way of stating that the Cramér function should be insensitive to the details of the production of pulses in the forcing range. It implies that A is an upper bound for the real

part of the σ_i's. Arranging the eigendirections $\boldsymbol{\Psi}_{ir}$ in order of decreasing Re σ_i, we are therefore led to identify $\mathbf{b}^0(\tau)$ with $\boldsymbol{\Psi}_{1r}(\tau)$. In the case of zero noise where we recover the deterministic solution of Sec. II [with $\boldsymbol{\xi}^0=\mathbf{0}$ in both Eqs. (3.5) and (4.1)], the time derivative $d\mathbf{b}^0/d\tau$ is also the solution of Eq. (4.1) with the same Lyapunov exponent as $\mathbf{b}^0$, $\sigma=A$ ($=A_0$ in this case). In this limit we would naturally define $\boldsymbol{\Psi}_{2r}(\tau)$ as $d\mathbf{b}^0/d\tau$. This property is lost in the more general situation of a nonvanishing noise, because $\boldsymbol{\xi}^0$ is not time invariant. What remains true, however, is the fact that $\mathbf{b}^0$ and $d\mathbf{b}^0/d\tau$ still span the set of ''coherent'' fluctuations which do not affect the shape of the pulse but modify its height and position.

By turning now our attention to the linear dynamics dual to Eq. (4.1) we shall come close to Eq. (3.6). Let us indeed consider the equation of motion

$$\frac{d\boldsymbol{\theta}}{d\tau} = -{}^t\mathcal{L}\boldsymbol{\theta}, \quad (4.4)$$

where in order to limit the proliferation of symbols, we keep the same notation $\boldsymbol{\theta}$ for the new auxiliary field, although it is only in particular circumstances, to be clarified below, related to the $\boldsymbol{\theta}$ of Eqs. (3.5) and (3.6). From Eq. (4.1) we get

$$\frac{d\boldsymbol{\theta}}{d\tau} = -{}^t\mathcal{M}\boldsymbol{\theta} - \partial_\mathbf{b}[(\mathbf{b}\cdot\mathbf{b})^{1/2}\boldsymbol{\theta}\cdot B\boldsymbol{\xi}^0]|_{\mathbf{b}^0}. \quad (4.5)$$

The dual dynamics enables one to construct a basis of left eigenvectors $\boldsymbol{\Psi}_{il}(\tau)$ (with $1\leq i\leq d$) satisfying

$$\boldsymbol{\Psi}_{il}(\tau+T) = e^{-\sigma_i T}\mathcal{T}_{+1}\boldsymbol{\Psi}_{il}(\tau), \quad (4.6)$$

as well as the following orthogonality conditions with the members of the first basis,

$$\boldsymbol{\Psi}_{il}(\tau)\cdot\boldsymbol{\Psi}_{jr}(\tau) = \delta_{ij}, \quad (4.7)$$

at every time. The vectors $\boldsymbol{\Psi}_{il}(0)$ are determined by diagonalizing the adjoint Floquet operator

$$^tU_T = \overrightarrow{\exp}\int_0^T {}^t\mathcal{L}d\tau\mathcal{T}_{+1}, \quad (4.8)$$

and enforcing the normalization condition (4.6) at time $\tau=0$ ($\overrightarrow{\exp}$) is now an antichronologically time-ordered product. We may note at this point that the first left eigenvector $\boldsymbol{\Psi}_{1l}$ is, in the generic case of nonzero noise, the only one to display the scaling behavior anticipated for $\boldsymbol{\theta}^0$ according to Eq. (3.14), since its Lyapunov exponent equals $-\sigma_1=-A$. We conclude that the auxiliary equation (3.6) in the restricted manifold of self-similar solutions is tantamount to the relation

$$\boldsymbol{\theta}^0(\tau) = \mu_1\boldsymbol{\Psi}_{1l}(\tau), \quad (4.9)$$

where the multiplicative constant μ_1 is nothing but the overlap $\boldsymbol{\theta}^0\cdot\mathbf{b}^0[=\mu_1\boldsymbol{\Psi}_{1l}(\tau)\cdot\boldsymbol{\Psi}_{1r}(\tau)=\mu_1]$, which was shown before to be indeed a conserved quantity. This claim is further confirmed by rewriting the original equation (3.6) as

$$\frac{d\boldsymbol{\theta}}{d\tau} = -{}^{t}\mathcal{M}\boldsymbol{\theta} - (\boldsymbol{\theta}\cdot B\,{}^{t}B\,\boldsymbol{\theta})\mathbf{b} - (\mathbf{b}\cdot\mathbf{b})\boldsymbol{\theta}\cdot\frac{1}{2}[(\partial_{\mathbf{b}}B)\,{}^{t}B$$

$$+ B(\partial_{\mathbf{b}}{}^{t}B)]\boldsymbol{\theta}$$

$$= -{}^{t}\mathcal{M}\boldsymbol{\theta} - (\boldsymbol{\theta}\cdot B\,{}^{t}B\,\boldsymbol{\theta})\mathbf{b} - (\mathbf{b}\cdot\mathbf{b})\boldsymbol{\theta}\cdot(\partial_{\mathbf{b}}B)\,{}^{t}B\,\boldsymbol{\theta}.$$

Putting back 0 superscripts and reintroducing $\boldsymbol{\xi}^{0}$ by using Eq. (3.12), we arrive at

$$\frac{d\boldsymbol{\theta}^{0}}{d\tau} = -{}^{t}\mathcal{M}\boldsymbol{\theta}^{0} - (\boldsymbol{\theta}^{0}\cdot B\boldsymbol{\xi}^{0})\frac{\mathbf{b}^{0}}{(\mathbf{b}^{0}\cdot\mathbf{b}^{0})^{1/2}}$$

$$- (\mathbf{b}^{0}\cdot\mathbf{b}^{0})^{1/2}\partial_{\mathbf{b}}(\boldsymbol{\theta}^{0}\cdot B\boldsymbol{\xi}^{0}), \tag{4.10}$$

which shows that $\boldsymbol{\theta}^{0}$ obeys the dual dynamics defined by Eq. (4.4).

Having interpreted Eq. (3.6) as a condition of self-consistency for the conjugate momentum $\boldsymbol{\theta}$ expressed by Eq. (4.9), we could contemplate the following Newton-like procedure for catching numerically self-similar instantons. First make a guess for $\boldsymbol{\xi}$ in the form of a traveling wave $[\boldsymbol{\xi}^{in}(\tau + T) = \mathcal{T}_{+1}\boldsymbol{\xi}^{in}(\tau)]$, integrate Eq. (3.6) forward in time in order to determine the asymptotic traveling state reached by $\mathbf{b}$ in the prescribed configuration of the noise. Then compute $\boldsymbol{\Psi}_{1l}$ from the diagonalization of ${}^{t}U_{T}$ [or from running Eq. (4.4) backward in time in order to let emerge the eigendirection of lowest growth rate], employ Eq. (4.9) for producing a new configuration of $\boldsymbol{\theta}$ (and thereby $\boldsymbol{\xi}$), and iterate this loop many times at a fixed value of the overlap μ_{1} until convergence is achieved. However, two major difficulties call for an improvement of the method: they both have to do with the stability of the trajectory upon time reparametrization. First we do not know the speed (or the inverse period T^{-1}) of the final traveling wave that must carry together $\mathbf{b}$ and $\boldsymbol{\xi}$. Therefore, when performing the first step of the iterative loop, we must allow continuous time reparametrization of our Ansatz for the noise in order to fine tune the speeds of the two pulses formed by $\mathbf{b}$ and $\boldsymbol{\xi}$ and let both terms on the right hand-side of Eq. (3.5) always be relevant. It will be explained in Sec. IV B how this goal can be achieved in practice. The second difficulty is much more serious than the preceding one and in the way of getting around it resides perhaps the most tricky part of this work. The point is that traveling-wave solutions to Eqs. (3.5) and (3.6) may perfectly have a nonzero pseudoenergy $\mathcal{H}$, while we are looking for the particular ones with $\mathcal{H}=0$. We shall be able to fulfill asymptotically the two conditions $\mathbf{b}\cdot\boldsymbol{\theta}=\mu_{1}$ and $\mathcal{H}=0$, if and only if our iterative guess for $\boldsymbol{\theta}$ is constructed within a two-dimensional space rather than a unidimensional one as in the naive proposal made above. For this purpose, we are going to embed the linearized dynamics (4.1) into a new one which admits the time translation mode $d\mathbf{b}^{0}/d\tau$ as a true eigenstate of the same growth factor A as $\mathbf{b}^{0}$, restoring thereby the symmetries present in the absence of noise. We shall do that in the most economical way, from both formal and numerical points of view, by substituting $\boldsymbol{\Phi}_{2r}=d\mathbf{b}^{0}/d\tau$ to $\boldsymbol{\Psi}_{2r}$, i.e., the eigendirection along which the fluctuations of $\mathbf{b}$ around $\mathbf{b}^{0}$ are the less stable.

The left eigenvector $\boldsymbol{\Psi}_{2l}$ is first rescaled as $\boldsymbol{\Phi}_{2l}$ $=\boldsymbol{\Psi}_{2l}/\boldsymbol{\Psi}_{2l}\cdot\boldsymbol{\Phi}_{2r}$ (which makes sense as long as $\boldsymbol{\Psi}_{2l}\cdot\boldsymbol{\Phi}_{2r}$

$\neq 0$, a condition always found to be satisfied in practice), so that $\boldsymbol{\Phi}_{2l}$ has a unit overlap with $\boldsymbol{\Phi}_{2r}$, while being orthogonal to all other right eigenvectors $\boldsymbol{\Psi}_{ir}$ with $i\neq 2$ (which will be noted $\boldsymbol{\Phi}_{ir}$ from now on). One then considers the modified linear dynamics:

$$\frac{d\delta\mathbf{b}}{d\tau} = \tilde{\mathcal{L}}\delta\mathbf{b} = \mathcal{L}\delta\mathbf{b} + (\mathbf{b}^{0}\cdot\mathbf{b}^{0})^{1/2}(\boldsymbol{\Phi}_{2l}\cdot\delta\mathbf{b})B\frac{d\boldsymbol{\xi}^{0}}{d\tau}. \tag{4.11}$$

It is easily checked that $\boldsymbol{\Phi}_{2r}=d\mathbf{b}^{0}/d\tau$ obeys Eq. (4.11), since Eq. (3.5) yields upon time derivation

$$\frac{d\boldsymbol{\Phi}_{2r}}{d\tau} = \mathcal{L}\boldsymbol{\Phi}_{2r} + (\mathbf{b}^{0}\cdot\mathbf{b}^{0})^{1/2}B\frac{d\boldsymbol{\xi}^{0}}{d\tau} = \tilde{\mathcal{L}}\boldsymbol{\Phi}_{2r}. \tag{4.12}$$

It is also trivially seen that the other vectors $\boldsymbol{\Phi}_{ir}=\boldsymbol{\Psi}_{ir}$ for $i\neq 2$ keep the same evolution under Eq. (4.11) as under Eq. (4.1). The dual dynamics now reads

$$\frac{d\boldsymbol{\theta}}{d\tau} = -{}^{t}\tilde{\mathcal{L}}\boldsymbol{\theta} = -{}^{t}\mathcal{L}\boldsymbol{\theta} - (\mathbf{b}^{0}\cdot\mathbf{b}^{0})^{1/2}\left(\boldsymbol{\theta}\cdot B\frac{d\boldsymbol{\xi}^{0}}{d\tau}\right)\boldsymbol{\Phi}_{2l}. \tag{4.13}$$

It leads to a new family of left eigenvectors $\boldsymbol{\Phi}_{il}$, dual to the direct basis, whose second member $\boldsymbol{\Phi}_{2l}$ has been defined above and the others relate to their original counterparts $\boldsymbol{\Psi}_{il}$ as

$$\boldsymbol{\Phi}_{il} = \boldsymbol{\Psi}_{il} - (\boldsymbol{\Psi}_{il}\cdot\boldsymbol{\Phi}_{2r})\boldsymbol{\Phi}_{2l}. \tag{4.14}$$

Although the $\boldsymbol{\Phi}_{il}$'s were introduced as a rather formal trick, it should be emphasized that $\boldsymbol{\Phi}_{1l}$ and $\boldsymbol{\Phi}_{2l}$ have an appealing physical meaning. Parametrizing a perturbed trajectory for $\mathbf{b}$ as $\mathbf{b}=e^{\delta\ln b(\tau)}\mathbf{b}^{0}[\tau + \delta\tau(\tau)] + \delta\mathbf{b}_{inc}$, where the "incoherent" part of fluctuations $\delta\mathbf{b}_{inc}$ is bound to be a linear superposition of the less dangerous modes $\boldsymbol{\Phi}_{ir}$ for $i\geq 3$, one has indeed, to linear order in $\delta\mathbf{b}$,

$$\delta\ln b = \boldsymbol{\Phi}_{1l}\cdot\delta\mathbf{b}, \tag{4.15}$$

$$\delta\tau = \boldsymbol{\Phi}_{2l}\cdot\delta\mathbf{b}. \tag{4.16}$$

These two relations will be useful in the computation of quadratic fluctuations to be presented in Sec. V. They show that by projecting out the multidimensional fluctuation field $\delta\mathbf{b}$ onto the two vectors $\boldsymbol{\Phi}_{1l}$ and $\boldsymbol{\Phi}_{2l}$, one has access to the most relevant part of it affecting, respectively, the amplitude and the time delay of the pulse constituting the instanton. In terms of $\boldsymbol{\Phi}_{1l}$ and $\boldsymbol{\Phi}_{2l}$, the self-consistency condition (4.9) for $\boldsymbol{\theta}^{0}$ together with the requirement of zero pseudoenergy $\mathcal{H}$ take the following form:

$$\boldsymbol{\theta}^{0}(\tau) = \mu_{1}\boldsymbol{\Phi}_{1l}(\tau) + \mu_{2}(\tau)\boldsymbol{\Phi}_{2l}(\tau), \tag{4.17}$$

where

$$\mu_{2}(\tau) = \frac{1}{2}\boldsymbol{\theta}^{0}\cdot B\,{}^{t}B\,\boldsymbol{\theta}^{0} = \frac{1}{2}\boldsymbol{\xi}^{0}\cdot\boldsymbol{\xi}^{0}. \tag{4.18}$$

Since from Eq. (4.17), $\mu_{2}(\tau) = \boldsymbol{\Phi}_{2r}\cdot\boldsymbol{\theta}^{0}$, and from the equation of motion (3.6), $\boldsymbol{\Phi}_{2r}\cdot\boldsymbol{\theta}^{0} = \mathcal{H} + \frac{1}{2}\boldsymbol{\xi}^{0}\cdot\boldsymbol{\xi}^{0}$, the relation (4.18) is just a way of restating $\mathcal{H}=0$. That Eq. (4.9) implies Eq. (4.17) results from the general link between $\boldsymbol{\Psi}_{1l}$ and $\boldsymbol{\Phi}_{1l}$ [see Eq. (4.14)]. The reverse is true only under the supple-

mentary condition of constant $\mathcal{H}$ or $\mu_2(\tau) = C^{te} + \frac{1}{2}\boldsymbol{\xi}^0 \cdot \boldsymbol{\xi}^0$, which is guaranteed by Eq. (4.18). It is proven by checking that in that case $\boldsymbol{\theta}^0(\tau)$, as given by Eq. (4.17), obeys, as it should, Eq. (4.4),

$$\frac{d\boldsymbol{\theta}^0}{d\tau} = -{}^t\tilde{\mathcal{L}}\boldsymbol{\theta}^0 + \frac{d\mu_2}{d\tau}\boldsymbol{\Phi}_{2l}$$

$$= -{}^t\mathcal{L}\boldsymbol{\theta}^0 - (\mathbf{b}^0 \cdot \mathbf{b}^0)^{1/2}\left(\boldsymbol{\theta}^0 \cdot B\frac{d\boldsymbol{\xi}^0}{d\tau}\right)\boldsymbol{\Phi}_{2l} + \frac{d\mu_2}{d\tau}\boldsymbol{\Phi}_{2l}$$

$$= -{}^t\mathcal{L}\boldsymbol{\theta}^0 + \frac{d}{d\tau}\left(\mu_2 - \frac{1}{2}\boldsymbol{\xi}^0 \cdot \boldsymbol{\xi}^0\right)\boldsymbol{\Phi}_{2l}$$

$$= -{}^t\mathcal{L}\boldsymbol{\theta}^0 + \frac{d\mathcal{H}}{d\tau}\boldsymbol{\Phi}_{2l}.$$

The great advantage of Eqs. (4.17) and Eq. (4.18) with respect to (4.9) is that this couple of equations lends itself to iterative procedures leading inexorably to a fixed point of zero pseudoenergy, a task seemingly out of reach before. There is some unavoidable arbitrariness in the construction proposed here, concerning in particular the definition of the vector $\boldsymbol{\Phi}_{2l}$, about which the reader may feel a little uncomfortable. We suspect that these unwanted features do not affect the final results since the original equations to be solved as well as the corresponding conserved quantities all have a clear mathematical definition where $\boldsymbol{\Phi}_{1l}$ and $\boldsymbol{\Phi}_{2l}$ merge together into $\boldsymbol{\Psi}_{1l}$.

B. Practical implementing and results

The action density $s_0(z)$ could be computed successfully for the three stochastic models defined in Sec. II using the iterative scheme outlined before. The shell lattice was first mapped onto a circle of d sites, with d typically ranging between 20 and 30. Finite size effects turn out to be completely negligible at such lengths of the chain, due to the strongly localized structure of the instantons. To start the computation, we make a guess for both the unit field $\mathbf{C}(\tau) = \mathbf{b}(\tau)/(\mathbf{b}\cdot\mathbf{b})^{1/2}(\tau)$ and the noise $\boldsymbol{\xi}(\tau)$ called henceforth $\mathbf{C}^{in}(\tau)$ and $\boldsymbol{\xi}^{in}(\tau)$. They are such that

$$C_{n+1}^{in}(\tau + T^{in}) = C_n^{in}(\tau), \qquad \xi_{n+1}^{in}(\tau + T^{in}) = \xi_n^{in}(\tau), \quad (4.19)$$

and

$$C_{n+d}^{in}(\tau) = C_n^{in}(\tau), \qquad \xi_{n+d}^{in}(\tau) = \xi_n^{in}(\tau). \quad (4.20)$$

Furthermore, the noise is normalized in such a way that the overlap $\mathbf{b}\cdot\boldsymbol{\theta} = \mathbf{C}\cdot B^{-1}[\mathbf{C}]\boldsymbol{\xi}$ takes on a prescribed value μ_1 held as a control parameter during all the steps of the computation. A possible and convenient choice would be for instance $\mathbf{C}^{in}(\tau) = \mathbf{C}^0(\tau)$, where $\mathbf{C}^0(\tau)$ is the deterministic solution of the scaling exponent z_0, and $\boldsymbol{\xi}^{in}(\tau) = \mu_1(\mathbf{b}^0 \cdot \mathbf{b}^0)^{1/2} B[\mathbf{C}^0]\boldsymbol{\Phi}_{1l}^0(\tau)$, where $\boldsymbol{\Phi}_{1l}^0(\tau)$ is the left eigenvector dual to $\mathbf{b}^0(\tau)$, i.e., in the absence of noise. Figure 1 shows how both vectors $\boldsymbol{\Phi}_{1l}^0$ and $\boldsymbol{\Phi}_{2l}^0$ look like at a given time. Their shapes will in fact evolve little as we let the scaling exponent z depart from z_0.
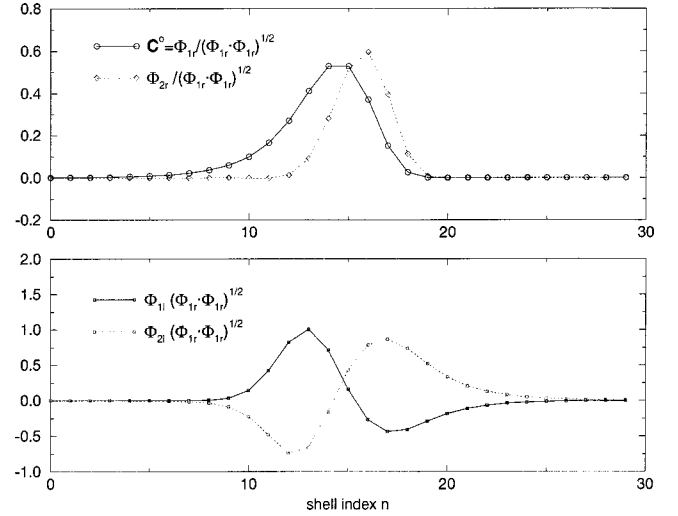

FIG. 1. On the upper (lower) picture we plot the configurations at a given instant of the right (left) eigenmodes in the subspace of maximum Lyapunov exponent A_0 around the deterministic solution.

In order to allow time reparametrization of the trajectory, we first get an estimate of the instantaneous position of the pulse along the shell axis in our trial configuration by computing the following quantity:

$$n^{in}(\tau) = \sum_{n=0}^{d-1} n[d][C_n^{in}(\tau)]^2. \quad (4.21)$$

The notation $n[d]$ recalls that, due to cyclic boundary conditions, the shell index n is now only defined modulo d and that in practice a continuous determination of this integer should be adopted close to the center of the pulse which contributes mostly to the right-hand side of Eq. (4.21). One has by construction $n^{in}(\tau + T^{in}) = n^{in}(\tau) + 1 \pmod d$. Having recorded $n^{in}(\tau)$ and $\boldsymbol{\xi}^{in}(\tau)$ during a whole period T^{in}, we integrate forward in time the nonlinear evolution equation for $\mathbf{C}$ deduced from Eq. (2.11) by projecting out the longitudinal part of its right-hand side:

$$\frac{d\mathbf{C}}{d\tau} = \{\mathbf{N}[\mathbf{C}](\tau) + B[\mathbf{C}](\tau)\boldsymbol{\xi}^{in}(\tau')\}_{\perp}. \quad (4.22)$$

Note that the subindex Γ disappeared from the nonlinear kernel $\mathbf{N}_\Gamma$ because the Ito-drift term being linear in Γ does not matter in the computation of the action to leading order (we shall see in the next section how to handle it to next to leading order). The most salient feature of Eq. (4.22) is that the noise configuration is evaluated in relation not to the time τ but rather to the actual instantaneous position of the pulse. This means that the time $\tau'(\tau)$ is automatically delayed or advanced with respect to τ, according to the recipe

$$n^{in}(\tau') = n(\tau) \quad \text{or} \quad \tau' = (n^{in})^{-1}[n(\tau)]. \quad (4.23)$$

After integrating Eq. (4.22) long enough, a new traveling wave state $\mathbf{C}^{out}(\tau), \boldsymbol{\xi}^{out}(\tau) = \boldsymbol{\xi}^{in}[\tau'(\tau)]$ will usually emerge of period T^{out}, possibly different from T^{in}, and an averaged growth factor

$$A^{out}=\frac{1}{T^{out}}\int_{\tau}^{\tau+T^{out}}(\mathbf{N}[\mathbf{C}^{out}]+B[\mathbf{C}^{out}]\boldsymbol{\xi}^{out})\cdot\mathbf{C}^{out}d\tau.$$

(4.24)

The vectors $\boldsymbol{\Psi}_{1l}(\tau)$, $\boldsymbol{\Psi}_{2l}(\tau)$ are then identified as the two eigenvectors of $^tU_{T^{out}}$ [defined in (4.8)] of the smallest (real negative) Lyapunov coefficient and the corresponding $\boldsymbol{\Phi}_{1l}(\tau),\boldsymbol{\Phi}_{2l}(\tau)$ constructed as linear combinations of them obeying for all times the following relations:

$$\boldsymbol{\Phi}_{1l}\cdot\mathbf{b}^{out}=\boldsymbol{\Phi}_{2l}\cdot\frac{d\mathbf{b}^{out}}{d\tau}=1,$$

$$\boldsymbol{\Phi}_{2l}\cdot\mathbf{b}^{out}=\boldsymbol{\Phi}_{1l}\cdot\frac{d\mathbf{b}^{out}}{d\tau}=0.$$

Finally, the trial noise configuration is renewed as $\boldsymbol{\xi}^{in}(\tau)=(\mathbf{b}^{out}\cdot\mathbf{b}^{out})^{1/2t}B[\mathbf{C}^{out}]\boldsymbol{\theta}^{in}$ with

$$\boldsymbol{\theta}^{in}(\tau)=\mu_1\boldsymbol{\Phi}_{1l}(\tau)+\mu_2(\tau)\boldsymbol{\Phi}_{2l}(\tau),$$

(4.25)

where $\mu_2(\tau)$ is determined upon imposing the condition of zero pseudoenergy on the trial solution $[\boldsymbol{\theta}^{in}(\tau),\mathbf{b}^{out}(\tau)]$

$$\boldsymbol{\theta}^{in}\cdot\mathbf{N}[\mathbf{C}^{out}]+\frac{1}{2}(\mathbf{b}^{out}\cdot\mathbf{b}^{out})\boldsymbol{\theta}^{in}\cdot B[\mathbf{C}^{out}]^tB[\mathbf{C}^{out}]\boldsymbol{\theta}^{in}=0.$$

(4.26)

After setting $\mathbf{b}^{in}(\tau)=\mathbf{b}^{out}(\tau)$, we are ready to repeat the operations described above as many times as needed until a fixed point of the transformation [such that $\mathbf{b}^{out}(\tau)=\mathbf{b}^{in}(\tau)$ and $\boldsymbol{\xi}^{in}(\tau)=\boldsymbol{\xi}^{out}(\tau)$] is reached, which solves the problem. The good stability properties of the algorithm, as well as its iterative character, authorize a rather unsophisticated handling of issues raised by the time discretization. As required by the Ito convention, the equation of motion (4.22) was integrated using a first-order Euler scheme with a time step $\Delta\tau=T^{in}/N$ about 350 times smaller than the period. The time τ' was approximated as the multiple of $\Delta\tau$ making the relation (4.23) best satisfied. Similarly no higher-order interpolation scheme was devised for estimating with accuracy the output period T^{out}: it was again simply approximated as the multiple of $\Delta\tau$ making periodicity conditions (4.19) best satisfied for the output. However, the time step $\Delta\tau$ was changed at each iteration of the loop so to maintain the time resolution N constant. The efficiency of the method was greatly improved when seeking solutions of exponents z far from z_0 by increasing z gradually (through an increase of the control parameter μ_1) using as a first guess solutions of a lower but close scaling exponent z'. In this way convergence toward satisfactory self-similar solutions (of exponent z varying by less than 10^{-5} under iteration and pseudoenergy $\mathcal{H}\leq10^{-5}$) was attained in no more than 20 iterations.

We turn now to the presentation of our results. Figure 2 shows the action density $s_0(z)$ for the three models (i), (ii), and (iii) defined in Sec. II. Values of Γ were adjusted in order to provide the same curvature of $s_0(z)/\Gamma$ at the bottom of the curves, reached evidently at $z=z_0$. We see that the variations of the zeroth-order action get sharper on the $z>z_0$ side (the only one displayed in Fig. 2), as one goes from model (i) to model (iii). Figures 3, 4, and 5, referring, respec-
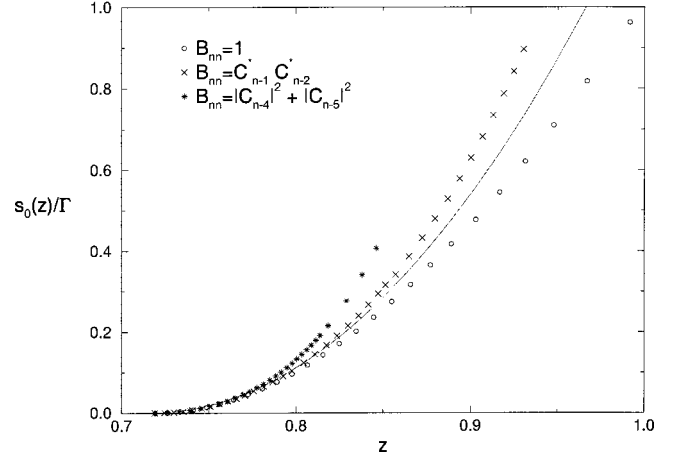

FIG. 2. Evolution of the normalized action per unit cascade step $s_0(z)/\Gamma$ as a function of the effective scaling exponent z for the three models studied in this paper. As a guide for the eyes we show the parabola (solid line) "tangent" to the curves at the deterministic minimum $z_0=0.72$.

tively, to models (i), (ii), and (iii), show the normalized coherent field $\mathbf{C}$ and the random force $B\boldsymbol{\xi}$ at increasing values of z (0.75, 0.85, and 0.95). In all cases the random force is found to be negative at the leading edge of the pulse, in agreement with the physical picture advocated in [5]: growth can be enhanced only by frustrating the energy transfer processes. For model (iii), the coherent field itself gets negative at the forefront: noise in that case just helps to prepare the system in an initial condition consisting of a pulse and a negative well in front of it, which then collide. An interesting upshot of our computations is that models like (ii) or (iii) involving only a local coupling between $\mathbf{b}$ and $\boldsymbol{\xi}$ escape the disaster met in the framework of model (i), namely a crossover toward an asymptotic linear growth of $s_0(z)$ with z, already perceptible in Fig. 2. Such a behavior forbids the existence of velocity moments at arbitrary orders and is, thus, clearly undesirable. It turns out that the whole shape of
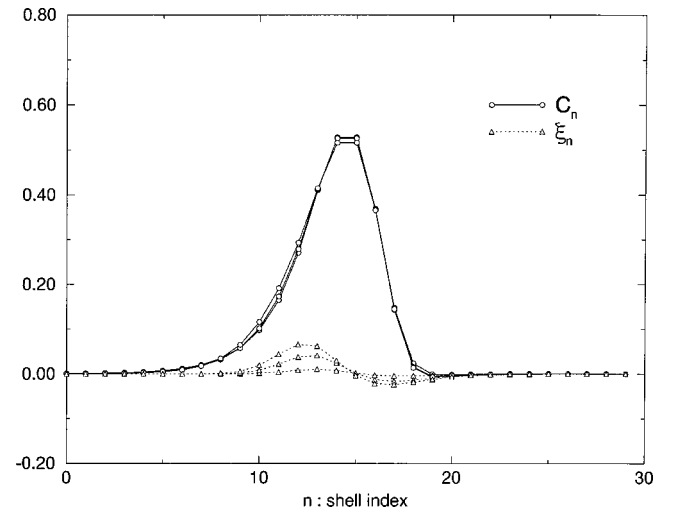

FIG. 3. Configurations of the normalized coherent field $\mathbf{C}$ and the random force $B\boldsymbol{\xi}$ for three instantons of exponents equal to $z=0.75,0.85,0.95$, obtained with the model (i) (according to the nomenclature defined in the text). Note that the $\mathbf{C}$ field is only slightly deformed as z increases.
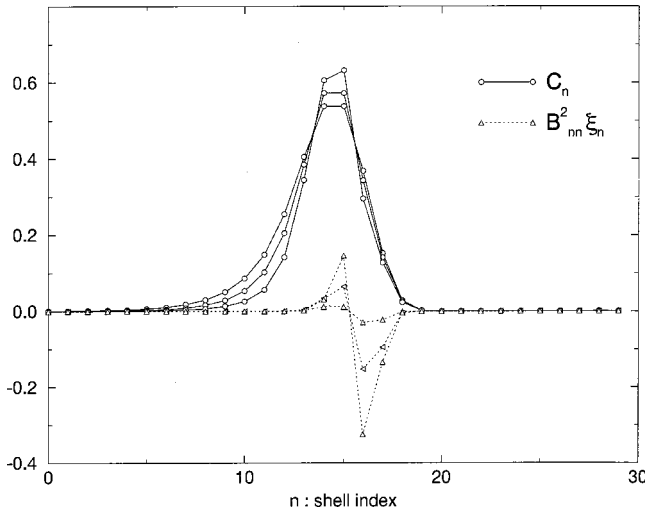
FIG. 4. Same as in Fig. 3 but for the model (ii). Note the more pronounced deformation of **C** upon increasing z, with respect to the previous case.

$s_0(z)$ for model (i) can be pretty well understood from an adiabatic approximation, which is carried out in the Appendix A, where solutions of arbitrary scaling exponents are constructed using adequate time reparametrizations and dilations of the deterministic solution of scaling exponent z_0. The validity of this approximation for the model (i) is somehow obvious from Fig. 3, where it can be checked that instantons keep indeed almost the same shape, even for quite sizeable variations of z. Its failure in models (ii) and (iii) is probably due to too strong deformations of the solutions as z increases, again suggested by Figs. 4 and 5. The full nonlinear treatment of the problem proposed in this paper was, however, necessary to reach this quite fortunate conclusion.

V. THE EFFECT OF QUADRATIC FLUCTUATIONS

A. Formal considerations

In order to compute the first order (in Γ) correction to the action per unit cascade step [$s_1(z)$ in the expression (2.8)] of
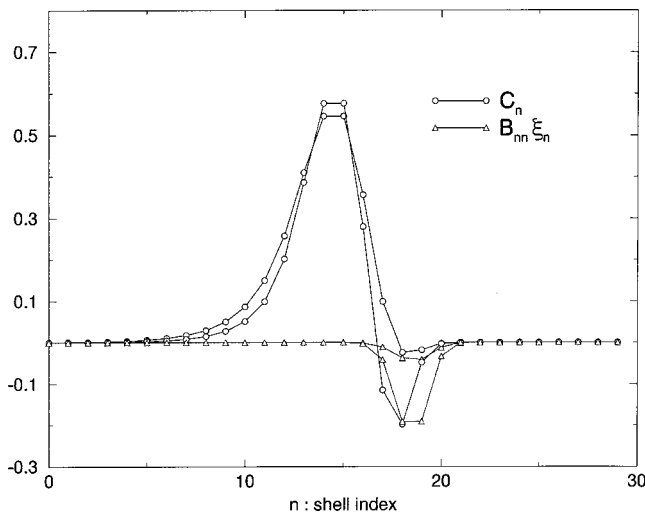

FIG. 5. Same as in Fig. 3 but for the model (iii) and only instantons of exponent $z = 0.75, 0.85$. The physical field now changes its sign at the leading edge of the pulse.

the density of probability $P_n(z)$, we have to expand the MSR action up to quadratic order in fluctuations $\delta \mathbf{b}$ around the extremal trajectory $\mathbf{b}^0(\tau)$ of scaling exponent z and then sum over them in a way that will be explained below. Since typical fluctuating paths are not differentiable but rather behave as Wiener paths with derivatives of the order $\frac{1}{2}$, we shall stick to time-discretized expressions in all the following manipulations of the path integral. For the sake of clarity, the superscript 0 referring to the extremal trajectory in the previous section Sec. IV will be taken away, whereas $\mathbf{b}_i, \theta_i$ will be short-hand notations for $\mathbf{b}^0(\tau_i = i\Delta\tau), \theta^0(\tau_i = i\Delta\tau)$, where $\delta\tau$ is the (small) time step used in the discretization.

We start from Eq. (3.1) and the representation (3.3) of the effective action $S[\mathbf{b}, \mathbf{p}]$, expand it to quadratic order in both fluctuations $\delta\mathbf{p}$ and $\delta\mathbf{b}$, and then integrate out the fluctuations of the auxiliary field. To begin, the time τ_f during which we let the system evolve will be equal to the time nT needed by the ideal instanton to perform n steps along the shell axis. The ideal initial and final configurations $\mathbf{b}_{in} = \mathbf{b}_0$ and $\mathbf{b}_f = \mathbf{b}_N$ describe then a pulse centered successively around the shells of index 0 and n. To quadratic order in deviations from the extremal trajectory, the probability of joining the perturbed endpoints $\mathbf{b}_{in} = \mathbf{b}_0 + \delta\mathbf{b}_0$ and $\mathbf{b}_f = \mathbf{b}_N + \delta\mathbf{b}_N$ in the time τ_f take the following expression:

$$P(\mathbf{b}_0 + \delta\mathbf{b}_0, 0; \mathbf{b}_N + \delta\mathbf{b}_N, \tau_f)$$

$$= e^{-ns_0(z)/\Gamma} \int \mathcal{D}\delta\mathbf{b} \exp(-\delta S[\delta\mathbf{b}] - \delta^2 S[\delta\mathbf{b}]), \quad (5.1)$$

where the measure of integration is defined as

$$\mathcal{D}\delta\mathbf{b} = \left(\frac{1}{2\pi\Gamma\,\Delta\tau}\right)^{dN/2} \frac{1}{(\mathbf{b}_0 \cdot \mathbf{b}_0)^{d/2}} \frac{1}{|\det B_0|}$$

$$\times \prod_{i=1}^{N-1} \left[\frac{d\,\delta\mathbf{b}_i}{(\mathbf{b}_i \cdot \mathbf{b}_i)^{d/2} |\det B_i|}\right], \quad (5.2)$$

the linear variation δS reduces to the boundary term

$$\delta S[\delta\mathbf{b}] = \frac{1}{\Gamma}\{\theta_{N-1} \cdot \delta\mathbf{b}_N - \theta_0 \cdot \delta\mathbf{b}_0\}, \quad (5.3)$$

and the quadratic one reads

$$\delta^2 S[\delta\mathbf{b}] = \frac{\Delta\tau}{2\Gamma} \sum_{i=0}^{N-1} \left[(\mathbf{b}_i \cdot \mathbf{b}_i)^{-1/2} B_i^{-1}\right.$$

$$\left. \times \left(\frac{\delta\mathbf{b}_{i+1} - \delta\mathbf{b}_i}{\Delta\tau} - \mathcal{A}_i \delta\mathbf{b}_i\right)^2 + \delta\mathbf{b}_i \cdot \mathcal{V}_i \delta\mathbf{b}_i\right.. \quad (5.4)$$

The drift and potential terms in Eq. (5.4) are found to be given by the following relations:

$$\mathcal{A}_i \delta\mathbf{b}_i = \mathcal{M}_i \delta\mathbf{b}_i + (\delta\mathbf{b}_i \cdot \partial_{\mathbf{b}_i})[(\mathbf{b}_i \cdot \mathbf{b}_i) B_i{}^t B_i \theta_i], \quad (5.5)$$

and

$$\boldsymbol{\delta b}_i \cdot \mathcal{V}_i \boldsymbol{\delta b}_i = -\boldsymbol{\theta}_i \cdot (\boldsymbol{\delta b}_i \cdot \partial_{\mathbf{b}_i}) \mathcal{M}_i \boldsymbol{\delta b}_i$$

$$-\frac{1}{2}\boldsymbol{\theta}_i \cdot (\boldsymbol{\delta b}_i \cdot \partial_{\mathbf{b}_i})^2 [(\mathbf{b}_i \cdot \mathbf{b}_i) B_i{}^t B_i \boldsymbol{\theta}_i], \quad (5.6)$$

where $\mathcal{M}$ is, as in previous sections, the Jacobian matrix of the nonlinear kernel $\mathbf{N}[\mathbf{b}]/(\mathbf{b} \cdot \mathbf{b})^{1/2}$.

Our task is to perform explicitly the integration over fluctuations $\boldsymbol{\delta b}_1, \ldots, \boldsymbol{\delta b}_{N-1}$ at intermediate steps in the path integral (5.1). First it will be convenient to get rid of the anisotropy of the ''mass'' tensor acting in the kinetic term of $\delta^2 S$ [21] by switching to normalized fluctuating fields defined as

$$\boldsymbol{\delta b}_i = (\mathbf{b}_i \cdot \mathbf{b}_i)^{1/2} B_i \mathbf{h}_i. \quad (5.7)$$

In this way the measure in the integral transforms into $[1/(\mathbf{b}_0 \cdot \mathbf{b}_0)^{d/2}](1/|\det B_0|) \mathcal{D}\mathbf{h}$ with

$$\mathcal{D}\mathbf{h} = \left(\frac{1}{2\pi\Gamma\,\Delta\tau}\right)^{dN/2} \prod_{i=1}^{i=N-1} d\mathbf{h}_i. \quad (5.8)$$

In performing this change of variables in $\delta^2 S$, we must pay attention to the fact that $\boldsymbol{\delta b}_{i+1} - \boldsymbol{\delta b}_i$, as well as $\mathbf{h}_{i+1} - \mathbf{h}_i$, are potentially of order $\Delta\tau^{1/2}$. One finds that up to $O(\Delta\tau^{3/2})$ corrections (negligible in the continuum limit), $\delta^2 S$ becomes

$$\delta^2 S[\mathbf{h}] = \frac{\Delta\tau}{2\Gamma} \sum_{i=0}^{N-1} \left[Q_i^{1/2} \left(\frac{\mathbf{h}_{i+1} - \mathbf{h}_i}{\Delta\tau} + \mathcal{D}_i \frac{\mathbf{h}_{i+1} + \mathbf{h}_i}{2} - \mathcal{A}_i' \mathbf{h}_i \right) \right]^2$$

$$+ \mathbf{h}_i \cdot \mathcal{V}_i' \mathbf{h}_i, \quad (5.9)$$

where

$$Q_i = \frac{1}{4} \left[1 + \left(\frac{\mathbf{b}_{i+1} \cdot \mathbf{b}_{i+1}}{\mathbf{b}_i \cdot \mathbf{b}_i} \right)^{1/2} {}^t B_{i+1} {}^t B_i^{-1} \right]$$

$$\times \left[1 + \left(\frac{\mathbf{b}_{i+1} \cdot \mathbf{b}_{i+1}}{\mathbf{b}_i \cdot \mathbf{b}_i} \right)^{1/2} B_i^{-1} B_{i+1} \right], \quad (5.10)$$

$$\mathcal{A}_i' = B_i^{-1} \mathcal{A}_i B_i, \quad (5.11)$$

$$\mathcal{V}_i' = (\mathbf{b}_i \cdot \mathbf{b}_i) {}^t B_i \mathcal{V}_i B_i, \quad (5.12)$$

and

$$\mathcal{D}_i = \frac{2}{\Delta\tau} [(\mathbf{b}_{i+1} \cdot \mathbf{b}_{i+1})^{1/2} B_{i+1}$$

$$+ (\mathbf{b}_i \cdot \mathbf{b}_i)^{1/2} B_i]^{-1} [(\mathbf{b}_{i+1} \cdot \mathbf{b}_{i+1})^{1/2} B_{i+1} - (\mathbf{b}_i \cdot \mathbf{b}_i)^{1/2} B_i]. \quad (5.13)$$

A few simplifications are now in order. On one hand we expand Q_i as $Q_i = 1 + \delta Q_i + O(\Delta\tau^2)$, where

$$\delta Q_i = \left(\frac{\mathbf{b}_{i+1} \cdot \mathbf{b}_{i+1}}{\mathbf{b}_i \cdot \mathbf{b}_i} \right)^{1/2} \frac{{}^t B_{i+1} {}^t B_i^{-1} + B_i^{-1} B_{i+1}}{2} - 1 \quad (5.14)$$

is of order $\Delta\tau$. Tracking $O(\Delta\tau)$ terms in $\delta^2 S$, we may replace Q_i by 1 everywhere in Eq. (5.9), except for the kinetic term $(1/2\Gamma)[(\mathbf{h}_{i+1} - \mathbf{h}_i) \cdot Q_i(\mathbf{h}_{i+1} - \mathbf{h}_i)/\Delta\tau]$, which accord-

ing to standard computation rules [18] in path integrals can be reduced to $(1/2\Gamma)[(\mathbf{h}_{i+1} - \mathbf{h}_i)^2/\Delta\tau] + \text{Tr}\,\delta Q_i$. On the other hand, exact ways of tracing out quadratic forms like $\delta^2 S$ are available only once they are written in terms of the midpoint field $(\mathbf{h}_{i+1} + \mathbf{h}_i)/2$ rather than $\mathbf{h}_i$ (which amounts to going back at this stage to the Stratonovich prescription). Again to order $\Delta\tau$, the substitution of $(\mathbf{h}_{i+1} + \mathbf{h}_i)/2$ to $\mathbf{h}_i$ in Eq. (5.9) is harmless except in the cross-product term $-(1/\Gamma)(\mathbf{h}_{i+1} - \mathbf{h}_i) \cdot \mathcal{A}_i' \mathbf{h}_i$ which gets into

$$-(1/\Gamma)(\mathbf{h}_{i+1} - \mathbf{h}_i) \cdot \mathcal{A}_i' \frac{\mathbf{h}_{i+1} + \mathbf{h}_i}{2} + \frac{\Delta\tau}{2} \text{Tr}\,\mathcal{A}_i'.$$

Setting things together, we arrive at the following expression for the transition probability in the neighborhood of the instanton:

$$P(\boldsymbol{\delta b}_{in} \to \boldsymbol{\delta b}_f, \tau_f) = \left| \det \frac{\partial\mathbf{h}}{\partial\mathbf{b}}(\tau_f) \right|$$

$$\times e^{-S_0(\tau_f)\Gamma} e^{-\mathcal{I}_1(\tau_f)} e^{1/\Gamma\{\boldsymbol{\theta}_{N-1} \cdot \boldsymbol{\delta b}_f - \boldsymbol{\theta}_0 \cdot \boldsymbol{\delta b}_{in}\}}$$

$$\times Z[\mathbf{h}_{in} \to \mathbf{h}_f, \tau_f], \quad (5.15)$$

where we defined

$$\mathcal{I}_1(\tau_f) = \frac{1}{2} \sum_{i=0}^{N-1} \text{Tr}\,\delta Q_i + \frac{\Delta\tau}{2} \sum_{i=0}^{N-1} \text{Tr}\,\mathcal{A}_i - dA\tau_f, \quad (5.16)$$

and the reduced path integral $Z[\mathbf{h}_{in} \to \mathbf{h}_f, \tau_f]$ as

$$Z[\mathbf{h}_{in} \to \mathbf{h}_f, \tau_f] = \int_{\mathbf{h}_0 = \mathbf{h}_{in}}^{\mathbf{h}_N = \mathbf{h}_f} \mathcal{D}\mathbf{h} \exp - \delta^2 S[\mathbf{h}] \quad (5.17)$$

with

$$\delta^2 S[\mathbf{h}] = \frac{\Delta\tau}{2\Gamma} \sum_{i=0}^{N-1} \left[\frac{\mathbf{h}_{i+1} - \mathbf{h}_i}{\Delta\tau} - \mathcal{B}_i \frac{\mathbf{h}_{i+1} + \mathbf{h}_i}{2} \right]^2$$

$$+ \frac{\mathbf{h}_{i+1} + \mathbf{h}_i}{2} \cdot \mathcal{V}_i' \frac{\mathbf{h}_{i+1} + \mathbf{h}_i}{2}, \quad (5.18)$$

and

$$\mathcal{B}_i = \mathcal{A}_i' - \mathcal{D}_i. \quad (5.19)$$

One easily shows that in the $\Delta\tau \to 0$ limit

$$\sum_i \text{Tr}\,\delta Q_i \to \text{Tr} \left[\ln \frac{(\mathbf{b}_N \cdot \mathbf{b}_N)^{1/2} B_N}{(\mathbf{b}_0 \cdot \mathbf{b}_0)^{1/2} B_0} \right] = dA\tau_f,$$

since the periodicity of the instanton implies that $\det B_N = \det B_0$, while

$$\Delta\tau \sum_i \text{Tr}\,\mathcal{A}_i \to \int_0^{\tau_f} \left\{ \partial_\mathbf{b} \cdot [(\mathbf{b} \cdot \mathbf{b}) B {}^t B \boldsymbol{\theta}] - \frac{\mathbf{N}[\mathbf{b}] \cdot \mathbf{b}}{(\mathbf{b} \cdot \mathbf{b})^{3/2}} \right\} d\tau.$$

However, the ensuing expression for $\mathcal{I}_1(\tau_f)$ is not yet complete to order $O(\Gamma^0)$. This is because we discarded the $O(\Gamma)$ Ito drift term in our computation of extremal trajectories. The small deviations induced by this term may be neglected

in $\mathcal{I}_1(\tau_f)$ and $-\ln Z[\mathbf{h}_{in}\rightarrow\mathbf{h}_f,\tau_f]$ which are already first-order corrections in a Γ expansion but they must be taken care of in the zeroth order term. Rather than $n[s_0(z)/\Gamma]$, it should read $S_\Gamma[\mathbf{b}_\Gamma^0]$, where the index Γ denotes a quantity or field evaluated in the presence of the Ito term specified in Eq. (2.10). To first order in Γ, we can take advantage of the extremum property of $\mathbf{b}_\Gamma^0$ and write down

$$S_\Gamma[\mathbf{b}_\Gamma^0]-S[\mathbf{b}^0]=S_\Gamma[\mathbf{b}_\Gamma^0]-S_\Gamma[\mathbf{b}^0]+S_\Gamma[\mathbf{b}^0]-S[\mathbf{b}^0]$$
$$\approx S_\Gamma[\mathbf{b}^0]-S[\mathbf{b}^0]$$
$$=\frac{1}{\Gamma}\int_0^{\tau_f}\boldsymbol{\theta}^0\cdot\frac{\mathbf{N}(\mathbf{b}^0)-\mathbf{N}_\Gamma[\mathbf{b}^0]}{(\mathbf{b}^0\cdot\mathbf{b}^0)^{1/2}}d\tau,$$

where the last identity just comes from the expression (3.4) of the action. Rearranging things under the assumption (satisfied by each of the particular models that we considered) that the entry B_{jk} of the matrix B involves homogeneous monomials of degree l built up only from components C_m with $m\neq j$ [one has $l=0$ for model (i) and $l=2$ for models (ii) and (iii) defined in Sec. II], one finds that $\mathcal{I}_1(\tau_f)$ in Eq. (5.15) should finally be understood as

$$\mathcal{I}_1(\tau_f)=\frac{(1-d)}{2}A\tau_f+\frac{(2l-3)}{4}\int_0^{\tau_f}\mathbf{b}^0\cdot B\,^tB\boldsymbol{\theta}^0 d\tau. \tag{5.20}$$

This preliminary work being done, the discussion will now concentrate on the reduced path integral $Z[\mathbf{h}_{in}\rightarrow\mathbf{h}_f,\tau_f]$. We first restrict our attention to the case of fixed endpoints $\mathbf{h}_{in}=\mathbf{h}_f=\mathbf{0}$. The instantons found in the previous sections are physically satisfactory only if the quadratic functional $\delta^2 S[\mathbf{h}]$ is positive for all $\{\mathbf{h}_i\}$ such that $\mathbf{h}_0=\mathbf{h}_N=\mathbf{0}$ (we shall see later on that this is not a sufficient condition in the present problem). According to standard results of functional analysis [19], positiveness of $\delta^2 S[\mathbf{h}]$ is tantamount to the absence of points conjugate to the origin during the whole time interval $[0,\tau_f]$. Recall that the definition of conjugate points goes as follows: d being the dimension of the space (here the number of shells) we construct d initial conditions $(\mathbf{h}_0^{(\alpha)},\mathbf{h}_1^{(\alpha)})$ such that

$$h_{0\beta}^{(\alpha)}=0,\qquad h_{1\beta}^{(\alpha)}=\Delta\tau\,\delta_{\alpha\beta}+O(\Delta\tau^2),$$

where β is a shell index running as α between 1 and d and we let them evolve under the Euler-Lagrange equations derived from $\delta^2 S[\mathbf{h}]$. The time $\tau_i=i\Delta\tau$ is said to be conjugate to the origin if the system formed by the d vectors $\mathbf{h}_i^{(\alpha)}$ gets degenerate there. One can build a matrix U_i such that $U_i^{\alpha\beta}=h_{i\alpha}^\beta$, in terms of which the initial conditions read

$$U_0=0,\qquad U_1=\Delta\tau+O(\Delta\tau^2), \tag{5.21}$$

while U_{i+1} (for $1\leq i\leq N-1$) is obtained from U_{i-1} and U_i through a matrix Euler-Lagrange equation, derived from Eq. (5.18) and conveniently cast into the following form:

$$\left(\frac{1}{\Delta\tau}+\frac{1}{2}\,^t\mathcal{B}_i\right)P_i-\left(\frac{1}{\Delta\tau}-\frac{1}{2}\,^t\mathcal{B}_{i-1}\right)P_{i-1}$$
$$=\frac{1}{2}\mathcal{V}_i'\frac{U_i+U_{i+1}}{2}+\frac{1}{2}\mathcal{V}_{i-1}'\frac{U_{i-1}+U_i}{2}, \tag{5.22}$$

where

$$P_i=\frac{U_{i+1}-U_i}{\Delta\tau}-\mathcal{B}_i\frac{U_i+U_{i+1}}{2} \tag{5.23}$$

can be seen as a matrix momentum. In the absence of conjugate points, $\det U_i$ never vanishes except at the origin and one gets the following simple expression for the reduced path integral, provided the $\Delta\tau\rightarrow 0$ limit is ultimately taken,

$$Z[\mathbf{h}_{in}=\mathbf{0}\rightarrow\mathbf{h}_f=\mathbf{0},\tau_f]=\left(\frac{1}{2\pi\Gamma}\right)^{d/2}\frac{1}{\sqrt{\det U(\tau_f)}}. \tag{5.24}$$

Details on this result, which may be found in many textbooks on path integrals [20–22], are provided in Appendix B. A very nice feature of the proof of the connection of the positiveness of $\delta^2 S[\mathbf{h}]$ with the absence of conjugate points is that it also provides an efficient way for computing the reduced path integral with $\mathbf{h}_f$ arbitrary (but still small naturally). Indeed the main idea consists of adding to $\delta^2 S[\mathbf{h}]$ a boundary term of the form

$$\delta^2 S'=-\frac{1}{2\Gamma}\sum_{i=0}^{N-1}(\mathbf{h}_{i+1}\cdot W_{i+1}\mathbf{h}_{i+1}-\mathbf{h}_i\cdot W_i\mathbf{h}_i),$$

where W is a symmetric matrix at all times and then selecting the right W such that $\delta^2 S+\delta^2 S'$ becomes a perfect square. In order to achieve this task, W_i must be a solution of a matrix Riccati equation (see again Appendix B for details) which, upon the substitution of a new unknown matrix U_i defined implicitly by the relation (for $0\leq i\leq N-1$)

$$\frac{1}{2}(W_iU_i+W_{i+1}U_{i+1})=\frac{U_{i+1}-U_i}{\Delta\tau}-\mathcal{B}_i\frac{U_i+U_{i+1}}{2}, \tag{5.25}$$

is found to be nothing but the matrix Euler equation (5.22). It follows that the result (5.24) may be extended to the case of an arbitrary final configuration $\mathbf{h}_f$ as

$$Z[\mathbf{h}_{in}=\mathbf{0}\rightarrow\mathbf{h}_f,\tau_f]=\left(\frac{1}{2\pi\Gamma}\right)^{d/2}\frac{1}{\sqrt{\det U(\tau_f)}}$$
$$\times\exp-\frac{1}{2\Gamma}\mathbf{h}_f\cdot W(\tau_f)\mathbf{h}_f, \tag{5.26}$$

where $U(\tau_f)$ and $W(\tau_f)$ are to be computed by letting both matrices evolve from $\tau=0$ to $\tau=\tau_f$ according to Eqs. (5.22) and (5.25). There are some subtleties about the choice of initial conditions and proper counting of the number of unknowns whose discussion we prefer to relegate to Appendix B.

B. A physical definition of $s_1(z)$

We are now in a good position to compute the next to leading order term $s_1(z)$ in the expansion of $-\lim_{n\to+\infty}(1/n)\ln P_n(z)$ in powers of Γ. We shall obtain an estimate for $P_n(z)$ by summing over all the trajectories which lead to the same growth of the pulse as the ideal instanton $\mathbf{b}^0(\tau)$ after n cascade steps. In the small Γ limit, all statistically relevant trajectories remain close to $\mathbf{b}^0(\tau)$ and we may define unambiguously their ''arrival'' time at the shell of index n as the first time τ_n such that

$$\mathbf{b}(\tau_n) = \mathbf{b}^0(\tau_n^0 = nT) + \boldsymbol{\delta b}', \qquad (5.27)$$

where $\boldsymbol{\delta b}'$ reduces to a linear combination of stable ''irrelevant'' modes $\boldsymbol{\Phi}_{ir}(\tau_n^0)$ for $i \geq 3$. Up to multiplicative factors growing at most algebraically with n, we can then write $P_n(z)$ as the following integral over the arrival time and the position of the endpoint

$$P_n(z) \approx \int P[\mathbf{b}^0(0) \to \mathbf{b}^0(\tau_n^0)$$
$$+ \boldsymbol{\delta b}', \tau_n]\delta(\boldsymbol{\Phi}_{1l}(\tau_n^0) \cdot \boldsymbol{\delta b}')\delta(\boldsymbol{\Phi}_{2l}(\tau_n^0) \cdot \boldsymbol{\delta b}')d\tau_n d\boldsymbol{\delta b}'. \tag{5.28}$$

The density of probability in the right-hand side of this expression is known from Eqs. (5.15) and (5.26), where τ_f should be taken equal to τ_n and $\boldsymbol{\delta b}_f$ equal to $\boldsymbol{\delta b} = \mathbf{b}(\tau_n) - \mathbf{b}^0(\tau_n)$. Calling $\delta\tau = \tau_n - \tau_n^0$ the time delay, we get the following relation between $\boldsymbol{\delta b}$ and $\boldsymbol{\delta b}'$, valid up to $O(\delta\tau^3)$ corrections:

$$\boldsymbol{\delta b} = \boldsymbol{\delta b}' + \mathbf{b}^0(\tau_n^0) - \mathbf{b}^0(\tau_n)$$
$$= \boldsymbol{\delta b}' - \delta\tau \frac{d\mathbf{b}^0}{d\tau}(\tau_n) + \frac{1}{2}\delta\tau^2 \frac{d^2\mathbf{b}^0}{d\tau^2}(\tau_n^0). \tag{5.29}$$

Note that $\delta\tau$ scales typically like $\sqrt{\Gamma}$ in the semiclassical limit. We may thus, to leading order, replace τ_n by τ_n^0 and identify $\boldsymbol{\delta b}$ with $\boldsymbol{\delta b}' - \delta\tau(d\mathbf{b}^0/d\tau)(\tau_n^0)$ everywhere in the integrand of the right-hand side of Eq. (5.28), except in $(1/\Gamma)[S_0(\tau_n) + \boldsymbol{\theta}^0(\tau_n) \cdot \boldsymbol{\delta b}]$ [the combination appearing in the exponential prefactor of Eq. (5.15)] which deserves more care. It follows from the definition of the action that [again up to $O(\delta\tau^3)$ corrections]

$$S_0(\tau_n) = S_0(\tau_n^0) + \delta\tau \frac{[\boldsymbol{\xi}^0(\tau_n)]^2}{2} - \frac{1}{2}\delta\tau^2 \boldsymbol{\xi}^0(\tau_n^0) \cdot \frac{d\boldsymbol{\xi}^0}{d\tau}(\tau_n^0), \tag{5.30}$$

and from Eq. (5.29) [together with the condition $\boldsymbol{\theta}^0(\tau_n^0) \cdot \boldsymbol{\delta b}' = 0$] that

$$\boldsymbol{\theta}^0(\tau_n) \cdot \boldsymbol{\delta b} = \delta\tau \frac{d\boldsymbol{\theta}^0}{d\tau}(\tau_n^0) \cdot \boldsymbol{\delta b}' - \delta\tau \boldsymbol{\theta}^0(\tau_n) \cdot \frac{d\mathbf{b}^0}{d\tau}(\tau_n)$$
$$+ \frac{1}{2}\delta\tau^2 \boldsymbol{\theta}^0(\tau_n^0) \cdot \frac{d^2\mathbf{b}^0}{d\tau^2}(\tau_n^0). \tag{5.31}$$

When summing these two equations, linear terms in $\delta\tau$ disappear as expected and we are left after some rearrangements with the remainder of quadratic order in fluctuations,

$$\frac{1}{\Gamma}\{S_0(\tau_n) + \boldsymbol{\theta}^0(\tau_n) \cdot \boldsymbol{\delta b}\} = \frac{1}{2}\delta\tau^2 \frac{d\boldsymbol{\theta}^0}{d\tau}(\tau_n^0) \cdot \frac{d\mathbf{b}^0}{d\tau}(\tau_n^0)$$
$$+ \delta\tau \frac{d\boldsymbol{\theta}^0}{d\tau}(\tau_n^0) \cdot \boldsymbol{\delta b}, \qquad (5.32)$$

where we set $\boldsymbol{\delta b} \equiv \boldsymbol{\delta b}' - \delta\tau(d\mathbf{b}^0/d\tau)(\tau_n^0)$, so that the time delay $\delta\tau$ is simply expressed in terms of $\boldsymbol{\delta b}$ as $\delta\tau = -\boldsymbol{\Phi}_{2l}(\tau_n^0) \cdot \boldsymbol{\delta b}$.

The end of our theoretical considerations is reached with the following expression for $P_n(z)$:

$$P_n(z) \approx e^{-ns_0(z)/\Gamma} \frac{e^{-\mathcal{I}_1(\tau_n^0)}}{\sqrt{\det U(\tau_n^0)}} \int \frac{e^{-(1/2\Gamma)\mathbf{h} \cdot \widetilde{W}(\tau_n^0)\mathbf{h}}}{(2\pi\Gamma)^{d/2}}$$
$$\times \delta(\boldsymbol{\Phi}_{1l}'(\tau_n^0) \cdot \mathbf{h})d\mathbf{h}, \qquad (5.33)$$

where $\boldsymbol{\Phi}_{1l}'(\tau) = (\mathbf{b}^0 \cdot \mathbf{b}^0)^{1/2}\,{}^t B \boldsymbol{\Phi}_{1l}(\tau)$ (so that $\boldsymbol{\Phi}_{1l}' \cdot \mathbf{h} = \boldsymbol{\Phi}_{1l} \cdot \boldsymbol{\delta b}$), $\widetilde{W} = W + \Delta W$, with W defined in Sec. V A and

$$\mathbf{h} \cdot \Delta W\mathbf{h} = -2(\boldsymbol{\Phi}_{2l}' \cdot \mathbf{h})(\mathbf{b}^0 \cdot \mathbf{b}^0)^{1/2} \frac{d\boldsymbol{\theta}^0}{d\tau} \cdot B\mathbf{h}$$
$$+ (\boldsymbol{\Phi}_{2l}' \cdot \mathbf{h})^2 \frac{d\boldsymbol{\theta}^0}{d\tau} \cdot \frac{d\mathbf{b}^0}{d\tau}. \qquad (5.34)$$

We see that the condition of positiveness of the matrix U must be supplemented by the condition of positiveness of the restriction W_1 of $\widetilde{W}$ to the $(d-1)$-dimensional space orthogonal to $\boldsymbol{\Phi}_{1l}'$, in order to make the instantons found in the preceding section physically meaningful. Provided these two requirements are met, $s_1(z)$ is obtained as

$$s_1(z) = \lim_{n\to+\infty}\frac{1}{n}\{\mathcal{I}_1(nT) + \tfrac{1}{2}\ln\det U(nT) + \tfrac{1}{2}\ln\det W_1(nT)\}, \tag{5.35}$$

which is the main result of this section.

Tracing back all the steps leading to Eq. (5.35), one could object to our starting point (5.28) the fact that fluctuations of the initial endpoint are not taken into account. This could be done at the expense of rather more cumbersome formulas for the reduced path integral $Z[\mathbf{h}(0) \to \mathbf{h}(\tau)]$ when both $\mathbf{h}(0)$ and $\mathbf{h}(\tau)$ do not vanish. However, we believe on physical grounds that the exploding associated with the instanton washes out any influence of the fluctuations at large scales on the part of the action scaling linearly with the number of steps n. Therefore expression (5.35) should be exact.

C. Practical implementing and results

The most difficult part of the computation of $s_1(z)$ lies in the evaluation of $\det U(\tau)$ and $\det W_1(\tau)$ (as defined in Sec. V B), which requires good control of all the eigenvalues of these two matrices. Numerical instabilities could be avoided for a time long enough to get a precise estimate of $(d/d\tau)\ln\det UW_1$ by using the exact expression of the ma-
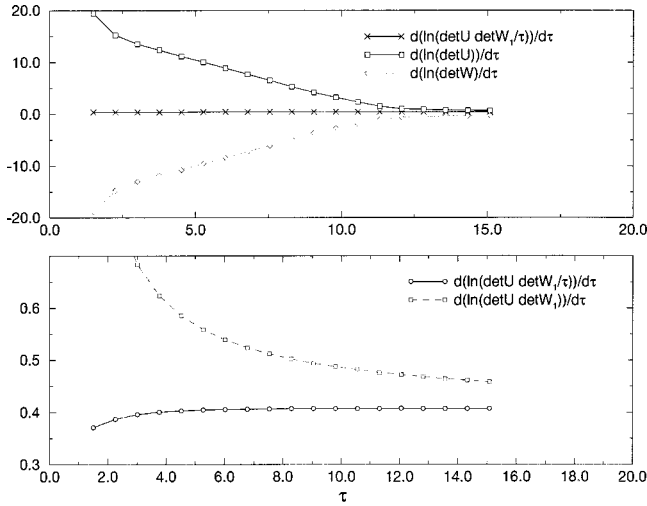
FIG. 6. Test for the convergence of several relevant quantities entering the calculation of the function $S_1(z)$. We show the case of the model (ii) at $z=0.8$.

FIG. 7. Graph (stars) of $s_0(z)/\Gamma + s_1(z)$ for $\Gamma=0.58$ and model (ii). The parabolic fit $S_{quad}=a(z-z_\star)^2$ yields $z_\star=0.74$ and $a=30$.

trix Euler equation (5.22) and the relation (5.25) between W and U. In this problem there are two Goldstone modes associated with uniform rescaling and time translation of the instanton: as a consequence, the matrix $(\mathbf{b}^0\cdot\mathbf{b}^0)^{1/2}BU(\tau)$ [respectively, $(\mathbf{b}^0\cdot\mathbf{b}^0)^{-1t}B^{-1}\widetilde{W}B^{-1}$] is expected to have two eigenvalues scaling like τ (respectively, like $1/\tau$) (in order to obtain the simplest transcription of these symmetries, one has to go back to the original fluctuation field $\delta\mathbf{b}=(\mathbf{b}^0\cdot\mathbf{b}^0)^{1/2}B\mathbf{h}$ and the change of variable influences eigenvalues of U and $\widetilde{W}$). When restricting $\widetilde{W}$ to the $(d-1)$-dimensional space orthogonal to $\Phi'_{1l}[\equiv(\mathbf{b}^0\cdot\mathbf{b}^0)^{1/2}B\Phi_{1l}]$, one loses one of the eigenvalues scaling like $1/\tau$, so that there remains an algebraic factor $\sqrt{\tau}$ in the product $\sqrt{\det U(\tau)}\sqrt{W_1(\tau)}$, which we had to take away by hand in order to make more conspicuous the leading exponential growth of this quantity. To give an idea of the accuracy of our procedure and confirm the soundness of the intricate formula (5.35) that was proposed for $s_1(z)$, we show in Fig. 6 the behavior of various relevant quantities in the case of model (ii), and for a moderate scaling exponent $z=0.8$. It is observed in the picture on the top that the logarithmic derivatives of $\det U$ and $\det W$ exhibit a linear behavior with almost opposite slopes. It can be shown by considering simpler and exactly solvable models for quadratic fluctuations without intershell couplings that this strange effect mostly reflects the stiff variations suffered by the noise variance on any shell, as the latter moves back from the leading edge of the instanton to its rear end. The argument is presented in Appendix C, since it may help the reader to get a feeling for the order of magnitudes at play in both U and W matrices.

It could be tempting at this level to approximate $s_1(z)$ as

$$\lim_{\tau\to\infty}\frac{d}{d\tau}\{\mathcal{I}_1+\tfrac{1}{2}\ln\det WU\}, \qquad (5.36)$$

This expression would come out if, without great physical justification, it were decided to sum over all positions of the final endpoint in the path-integral formulation in order to estimate the volume of the basin of attraction of the instan-
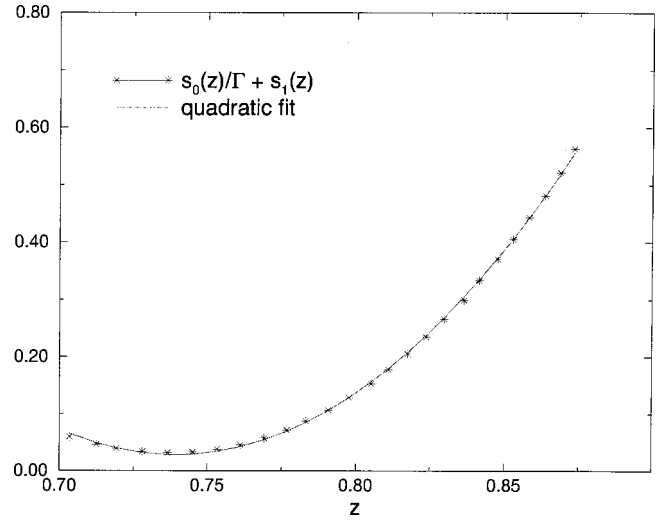
ton. We found, however, that the matrix momentum WU develops invariably a negative eigenvalue after some time, so that the projection onto the restricted phase space introduced in Sec. V B is a necessary step for restoring the statistical stability of the instanton. Further, even before this instability occurs, there was found to be a residual τ^2 term in $\ln\det WU$ which forbids any reliable estimate for $s_1(z)$ to be deduced from Eq. (5.36). The picture at the bottom of Fig. 6 shows by contrast that the more precise quantity $\det U\det W_1$ quickly settles to a perfect exponential growth, once algebraic transients have been factored out. Note that the positiveness of both U and W_1 could be checked in any instance.

In all the models that we investigated, we found that the first-order correction $s_1(z)$ to the action takes an approximate parabolic shape of positive or negative concavity, centered around a value of z different from z_0. In the case of model (ii), the concavity of $s_1(z)$ is opposite the one of $s_0(z)$ and the maximum of $s_1(z)$ is reached at a scaling exponent $z_1\approx0.6$, significantly lower than $z_0=0.72$. This means that the minimum of the total action density $s(z)=s_0(z)/\Gamma+s_1(z)$ [for values of Γ such that $s(z)$ remains concave as it should] is displaced toward the side of larger exponents, just as a result of fluctuations. The trend is just the opposite for the model (iii), where $s_1(z)$ presents this time the same concavity as $s_0(z)$ and a minimum on the left side of z_0. Figure 7 shows the graph of $s_0(z)/\Gamma+s_1(z)$ that is obtained for model (ii) and for the value $\Gamma=0.58$, which we believe to be of some relevance for the GOY model (see Sec. VI).

VI. COMPARISON WITH NUMERICAL DATA ON THE STATISTICS OF COHERENT EVENTS IN THE GOY MODEL

The systems we have analyzed here were introduced to describe inertial singular structures of the GOY model. To check their physical relevance, we first have to define a class of events observed in full simulations of the GOY model that is likely to be the best candidate for a description in terms of instantons. It is clear that relative maxima of the instanta-
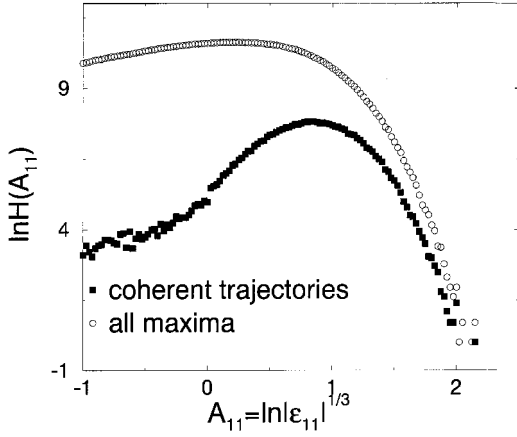
FIG. 8. Histograms of the energy flux in the log-log plot, involving all relative maxima of ϵ_n or only those associated with coherent events. The shell index $n = 11$, the Reynolds number Re is 10^8, and the number of TOTLS is 6×10^4.
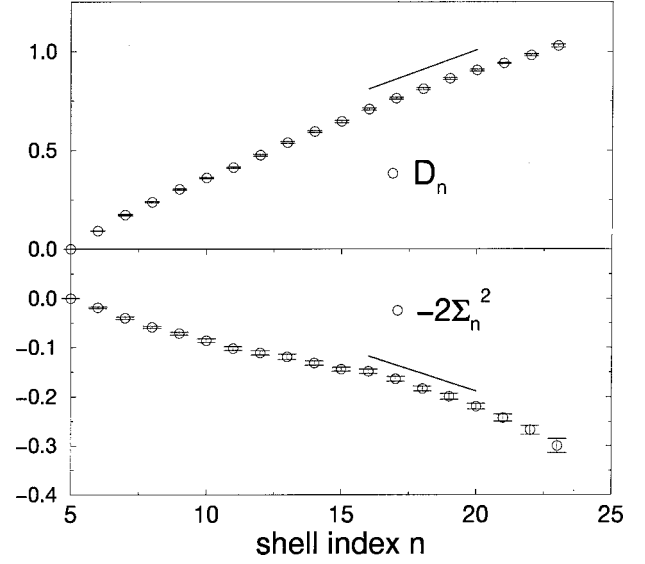

FIG. 9. The two quantities D_n and $-2\Sigma_n^2$ (encoding the Gaussian central part of the histogram of the growth variable $A_n - A_{n_0}$) vs n. The Reynolds number Re is 10^9 and the dissipative shell has index $n_d = 23$. The two pieces of straight line show the linear fits that were used to extract the values of $z_\star$ and a in the previscous range.

neous energy flux $\epsilon_n(t)$ [with $\epsilon_n = k_n^{-2} \text{Re}\{(1 - \epsilon)Q^2 b_{n-2}b_{n-1}b_n + b_{n-1}b_{n+1}b_n\}$] are useful observables for tracking the passage of coherent structures across the whole inertial range. But their total number is found to grow with n as $k_n^{2/3}$, due to the acceleration of time scales typical of the Kolmogorov energy cascade. One may consider that they develop on treelike patterns in the (n,t) plane, which are renewed at each turnover of the large scales (TOTLS). We say that such trees provide a realization of the propagation of a coherent event from shell n_0 to shell $n > n_0$, whenever the $n - n_0$ nodes of the tree closest in time to their supposedly common ancestor on the shell of lower index n_0 appear in the order of increasing shell index. In order to discard too weak, and therefore irrelevant, events, we imposed that ϵ_{n_0} be greater than half the mean energy flux. Figure 8 shows the logarithm of the histogram of the logarithmic amplitudes $A_n = \ln|\epsilon_n|^{1/3}$ for all relative maxima on one hand and for the restricted class of coherent events defined above on the other hand, with $n_0 = 5$ (far enough from the forcing range) and $n = 11$ (well in the inertial range). The Reynolds number of the simulation is $Re = 10^8$. Statistics have been run over 6×10^4 TOTLS, and on average there are three ''coherent lines'' for two TOTLS. We note that the statistics of coherent events is very close to log-normal for $|\epsilon_n| \gtrsim O(1)$.

The effective exponent z of a coherent burst after $n - n_0$ cascade steps is obtained via the relation $A_n = A_{n_0} + (n - n_0)(z - 2/3)\ln 2$. If anomalous scaling is preserved in the Re$\rightarrow \infty$ limit, the pdf of scaling exponents z should behave at large cascade lengths as $P_n(z) \sim e^{-ns(z)}$, where generically $s(z)$ will present a quadratic minimum at some $z_\star$, with an expansion around $z_\star$ that we write as $s(z) = a(z - z_\star)^2 + \cdots$. The histogram of the variable $A_n - A_{n_0}$ should consequently evolve, as $n - n_0$ increases, towards a Gaussian shape, whose center D_n and variance Σ_n^2 grow linearly with n and relate to $z_\star$ and a as

$$D_n \sim n\ln 2(z_\star - 2/3), \qquad \Sigma_n^2 \sim \frac{n}{2a}(\ln 2)^2. \qquad (6.1)$$

The actual behaviors of D_n and $-2\Sigma_n^2$, obtained from a very high Reynolds number simulation (Re$= 10^9$, which sets the dissipative scale at the shell index $n_d = \frac{3}{4}\ln_2 \text{Re} = 23$) are plotted in Fig. 9. Error bars were estimated by varying the range of the quadratic fit to the logarithm of the histogram of $A_n - A_{n_0}$, as well as the domain of initial amplitudes A_{n_0} used to construct this histogram. It appears that the two graphs are rather far from simple straight lines : this is especially true for the variance, whose graph from concave gets convex beyond the shell index 15. From the investigation of lower Reynolds numbers Re$= 10^8$ and 10^7 we could deduce that this transition occurs at a shell index n_c always of the order of $n_d - 8$ and defines a clear cut boundary between the inertial range and a surprisingly wide previscous range. We believe that the direct action of viscosity on intense bursts starts to show up only at the shell index $n_d - 3$, beyond which the local slope of the D_n graph ceases to vary and points to a value of the average growth exponent of coherent structures precisely equal to z_0. The fact that n_c lies rather far from n_d means that the cut off imposed by viscosity exerts a long-range influence on the statistics of the random environment seen by a coherent structure. A decent linear regime for both the drift and the variance is observed in the range $15 < n < 21$, from which we get the two estimates $a = 29 \pm 4$ and $z_\star = 0.74 \pm 3 \times 10^{-3}$. Assuming that the fitting range $10 < n < 16$ provides the best clue to the asymptotic scaling of the inertial range, one gets the second set of values $a = 45 \pm 6$ and $z_\star = 0.75 \pm 3 \times 10^{-3}$. It appears that the physics of the previscous range is quite well reproduced within our modeling (ii) of the incoherent background. By choosing $\Gamma = 0.58$ (a value hopefully small enough to fall within the range of validity of semiclassical approximations), one obtains, as Fig. 7 shows, an almost perfect parabolic shape of $s(z) = -[S_0(z)/\Gamma + S_1(z)]$, with a maximum reached at $z_\star = 0.74$ and a curvature $a = -2s''(z_\star) = 29$. However, the pa-

rameter Γ cannot be adjusted so as to account for the higher values of a and $z_\star$ characterizing the inertial range. It would seem that in this range of scales it gets necessary to assume some bias in the incoherent fluctuations boosting the increase of the renormalized value of $z_\star$ while keeping the noise width small.

VII. CONCLUSION

We have developed a general scheme for computing numerically self-similar instantons in scale-invariant stochastic dynamical systems. As concerns the physics of the GOY model, we believe that the bunch of results presented here gives strong support to the relevance of an approach focusing from the outset on structures in order to understand intermittency and treating the rest of the flow as a noise of weak amplitude. In particular the trend toward log-normal statistics of coherent structures is nicely recovered. The detailed study of various stochastic extensions of the GOY model shows that the resulting pdf of scaling exponents of singular structures is very sensitive to the hypothesis made on the coupling of noise to the velocity gradient fields.

We hope that our approach will be useful for attacking the 3D Navier-Stokes dynamics along similar lines, once an adequate decomposition of the flow into coherent and incoherent parts will have been introduced. An application of the method to Kraichnan's model of passive scalar advection formulated on a lattice of shells has already been attempted [22,23]. It has given encouraging results with regard to the validity of a semiclassical analysis, even in situations where a small parameter (like Γ in the present problem) is missing.

APPENDIX A

We carry out in this appendix the adiabatic approximation alluded to in Sec. IV B. We look for self-similar instantons within the restricted manifold of configurations of the type

$$\mathbf{b}(\tau)=e^{x(\tilde{\tau})}\mathbf{b}^0(\tilde{\tau}), \tag{A1}$$

where $\mathbf{b}^0(\tau)$ is the deterministic solution of scaling exponent z_0, $\tilde{\tau}$ can be thought of as a ''proper'' time referring to the actual position of the pulse. The two variables $\tau(\tilde{\tau})$ and $x(\tilde{\tau})$ parametrize then local changes of speed and amplitudes of the pulse, which keeps the same shape as in the absence of noise. Note that if Eq. (A1) is to represent a self-similar instanton of scaling exponent $z\neq z_0$, $x(\tilde{\tau})$ must obey the constraint

$$x(\tilde{\tau}+T_0)-x(\tilde{\tau})=(z-z_0)\ln Q. \tag{A2}$$

We plug now the Ansatz equation (A1) in the equation of motion (2.11) and project it onto the two directions $\mathbf{\Phi}_{1r}=\mathbf{b}^0$ and $\mathbf{\Phi}_{2r}=d\mathbf{b}^0/d\tau$. We get by doing so

$$\frac{d\tilde{\tau}}{d\tau}\frac{dx}{d\tilde{\tau}}=\mathbf{\Phi}_{1l}\cdot B\boldsymbol{\xi}, \tag{A3}$$

$$\frac{d\tilde{\tau}}{d\tau}-1=\mathbf{\Phi}_{2l}\cdot B\boldsymbol{\xi}. \tag{A4}$$

If the other dimensions of the configuration space are neglected, Eqs. (A3) and (A4) form a closed two-dimensional system, which may be rewritten as

$$\frac{dx}{d\tilde{\tau}}=\zeta_1, \tag{A5}$$

$$1-\frac{d\tau}{d\tilde{\tau}}=\zeta_2, \tag{A6}$$

where correlation functions of ζ_1 and ζ_2 read

$$\langle\zeta_i(\tilde{\tau})\zeta_j(\tilde{\tau}')\rangle=\frac{d\tau}{d\tilde{\tau}}V_{ij}\delta(\tilde{\tau}-\tilde{\tau}'), \qquad 1\leqslant i,j\leqslant2, \tag{A7}$$

with

$$V_{ij}=\mathbf{\Phi}_{il}\cdot B\,{}^tB\mathbf{\Phi}_{jl}. \tag{A8}$$

The Gaussian action density associated with one cascade step within this restricted stochastic system is given by

$$\tilde{s}=\frac{1}{2}\int_0^{T_0}d\tilde{\tau}\left(\frac{d\tau}{d\tilde{\tau}}\right)^{-1}\zeta_i(V^{-1})_{ij}\zeta_j. \tag{A9}$$

Once expressed in terms of the diffusing variables $x(\tilde{\tau})$ and $\tau(\tilde{\tau})$, it becomes

$$\tilde{s}=\frac{1}{2}\int_0^{T_0}d\tilde{\tau}\left\{\left(\frac{d\tau}{d\tilde{\tau}}\right)^{-1}[\dot{x}^2(V^{-1})_{11}+2\dot{x}(V^{-1})_{12}+(V^{-1})_{22}]\right.$$
$$\left.+\frac{d\tau}{d\tilde{\tau}}(V^{-1})_{22}-[\dot{x}(V^{-1})_{12}+(V^{-1})_{22}]\right\}. \tag{A10}$$

The extremization of $\tilde{s}$ with respect to $d\tau/d\tilde{\tau}$ leads to

$$\frac{d\tau}{d\tilde{\tau}}=\{(\dot{x}^2(V^{-1})_{11}+2\dot{x}(V^{-1})_{12}+(V^{-1})_{22}]V_{22}\}^{1/2}, \tag{A11}$$

and to an effective action for the remaining variable x

$$\tilde{s}_{eff}[x(\tilde{\tau})]=\int_0^{T_0}d\tilde{\tau}(\{[\dot{x}^2(V^{-1})_{11}+2\dot{x}(V^{-1})_{12}+(V^{-1})_{22}]$$
$$\times(V^{-1})_{22}\}^{1/2}-[\dot{x}(V^{-1})_{12}+(V^{-1})_{22}]). \tag{A12}$$

Assuming the coefficients V_{11}, V_{12}, and V_{22} to be almost constant inside the time interval T_0, one deduces an analytic

expression for $s_0(z)$ from $\tilde{s}_{eff}$ by just replacing in the integral $\dot{x}$ by $(z-z_0)\ln Q/T_0$ [which follows from Eq. (A2)]. One gets in particular for large enough $z-z_0$,

$$s_0(z) \sim (z-z_0)\ln Q \{[(V^{-1})_{11}(V^{-1})_{22}]^{1/2} - (V^{-1})_{12}\}, \tag{A13}$$

i.e, a linear behavior as observed for the true solution of model (i).

APPENDIX B

We derive the formal expression of the reduced path integral $Z[\mathbf{0} \to \mathbf{h}_f, \tau_f]$ given in Eq. (5.26) of Sec. V of the text. The proof is presented in many textbooks on path integrals but, as far as we know, always using a continuous definition of time. This leaves some ambiguity in the right equations that matrices U and W should obey, once time is discretized for computing purposes. We found that this issue is crucial mostly for evaluating W and preserving its symmetry properties. This is why we feel it useful to show how every step of the proof given in the continuum limit receives an exact transcription in the discrete time case.

We start from the quadratic functional

$$\delta^2 S[\mathbf{h}] = \frac{\Delta\tau}{2\Gamma} \sum_{i=0}^{i=N-1} \left\{ \left[\frac{\mathbf{h}_{i+1}-\mathbf{h}_i}{\Delta\tau} - \mathcal{B}_i\frac{\mathbf{h}_{i+1}+\mathbf{h}_i}{2}\right]^2 + \frac{\mathbf{h}_{i+1}+\mathbf{h}_i}{2}\cdot\mathcal{V}_i'\frac{\mathbf{h}_{i+1}+\mathbf{h}_i}{2}\right\}. \tag{B1}$$

Upon the addition of the boundary term

$$-(1/2\Gamma)\Sigma_{i=0}^{N-1}\{\mathbf{h}_{i+1}\cdot W_{i+1}\mathbf{h}_{i+1} - \mathbf{h}_i\cdot W_i\mathbf{h}_i\},$$

it becomes without any approximation

$$\delta^2 \tilde{S}[\mathbf{h}] = \frac{\Delta\tau}{2\Gamma} \sum_{i=0}^{i=N-1} \left(\left\{\tilde{Q}_i^{1/2}\left[\frac{\mathbf{h}_{i+1}-\mathbf{h}_i}{\Delta\tau} - \tilde{Q}_i^{-1}\right.\right.\right.$$
$$\left.\left.\times\left(\mathcal{B}_i - \frac{W_i+W_{i+1}}{2}\right)\frac{\mathbf{h}_{i+1}+\mathbf{h}_i}{2}\right]\right\}^2$$
$$+ \frac{\mathbf{h}_{i+1}+\mathbf{h}_i}{2}\cdot\tilde{\mathcal{V}}_i\frac{\mathbf{h}_{i+1}+\mathbf{h}_i}{2}\right), \tag{B2}$$

where

$$\tilde{Q}_i = 1 - \frac{\Delta\tau}{4}(W_{i+1}-W_i) \tag{B3}$$

and

$$\tilde{\mathcal{V}}_i = \mathcal{V}_i' + {}^t\mathcal{B}_i\mathcal{B}_i - \frac{W_{i+1}-W_i}{2} - \left({}^t\mathcal{B}_i - \frac{W_i+W_{i+1}}{2}\right)$$
$$\times\tilde{Q}_i^{-1}\left(\mathcal{B}_i - \frac{W_i+W_{i+1}}{2}\right). \tag{B4}$$

We see that $\delta^2\tilde{S}[\mathbf{h}]$ reduces to the time integral of a single (positive) square, if and only if W_i is such that for all $0\leq i \leq N-1$

$$\mathcal{V}_i' + {}^t\mathcal{B}_i\mathcal{B}_i - \frac{W_{i+1}-W_i}{2} - \left({}^t\mathcal{B}_i - \frac{W_i+W_{i+1}}{2}\right)$$
$$\times\tilde{Q}_i^{-1}\left(\mathcal{B}_i - \frac{W_i+W_{i+1}}{2}\right) = 0. \tag{B5}$$

We note that Eq. (B5) forces W_i to remain symmetric for all time, provided that W_0 (arbitrary at this stage) is chosen to be such. In order to solve the above Ricatti matrix equation, one makes the following change of matrix variable:

$$\left(\mathcal{B}_i + \frac{W_i+W_{i+1}}{2}\right)\left(\frac{U_i+U_{i+1}}{2}\right) = \tilde{Q}_i\frac{U_{i+1}-U_i}{\Delta\tau}. \tag{B6}$$

From the expression (B3) of $\tilde{Q}_i$, it is easily shown that Eq. (B6) is equivalent to Eq. (5.25) quoted in the text. Furthermore, by multiplying both sides of Eq. (B5) by $(U_i+U_{i+1})/2$ on the right, one gets for $0\leq i \leq N-1$

$$\frac{W_{i+1}U_{i+1}-W_iU_i}{\Delta\tau} = -{}^t\mathcal{B}_i\frac{U_{i+1}-U_i}{\Delta\tau}$$
$$+ ({}^t\mathcal{B}_i\mathcal{B}_i + \mathcal{V}_i')\frac{U_i+U_{i+1}}{2}. \tag{B7}$$

By half-summing the two relations yielded by Eq. (B7) at subsequent values $i-1$ and i of the temporal index (with then $1\leq i \leq N-1$), and using Eq. (5.25) after noticing that

$$\frac{W_{i+1}U_{i+1}-W_{i-1}U_{i-1}}{2\Delta\tau}$$
$$= \frac{(W_{i+1}U_{i+1}+W_iU_i)-(W_iU_i+W_{i-1}U_{i-1})}{2\Delta\tau},$$

one can eliminate W and check that U obeys the matrix Euler equation (5.22), as promised in the text.

So far, we have proven that, as long as the matrix U may be inverted, the positiveness of $\delta^2 S$ is guaranteed, since in that case the matrix W exists at all times [from Eq. (B6)] and allows one to transform the initial quadratic form into the time integral of a single square. We show now how these matrices lead to a compact expression of $Z[\mathbf{h}_0=\mathbf{0}\to\mathbf{h}_f, \tau_f]$. We first note that Eqs. (B6) and (B7) provide $2N$ relations for $2(N+1)$ unknowns $\{U_0, \ldots, U_N\}, \{W_0, \ldots, W_N\}$. This gives much freedom in the choice of W_0 and U_0. In the particular case of $\mathbf{h}_0=\mathbf{0}$, it is convenient to set $U_0=0$ and $W_0U_0=1$ (which should be understood as the limit as $\epsilon \to 0^+$ of $U_0=\epsilon$ and $W_0=\epsilon^{-1}$, so that W_0 is indeed symmetric). A quick inspection of Eqs. (B6) and (B7) reveals that U_i and W_i behave then respectively as $i\Delta\tau$ and $(i\Delta\tau)^{-1}$ to leading order in $\Delta\tau$ for $1\leq i \leq N$. One has, for instance, the exact result $W_1=(\Delta\tau)^{-1} - (\mathcal{B}_0 + {}^t\mathcal{B}_0)/2 + ({}^t\mathcal{B}_0\mathcal{B}_0 + \mathcal{V}_0')$. Recall that the quantity we wish to estimate reads now

$$Z[\mathbf{0} \to \mathbf{h}_f, \tau_f] = e^{-(1/2\Gamma)\mathbf{h}_f \cdot W_N \mathbf{h}_f}$$

$$\times \int \mathcal{D}\mathbf{h} \, \delta^d(\mathbf{h}_N - \mathbf{h}_f) e^{-(1/2) \sum_{i=0}^{N-1} \boldsymbol{\psi}_{i+1} \cdot \tilde{Q}_i \boldsymbol{\psi}_{i+1}}, \tag{B8}$$

where we defined the new field $\boldsymbol{\psi}_{i+1}$ (for $0 \leq i \leq N-1$) as

$$\boldsymbol{\psi}_{i+1} = \mathbf{h}_{i+1} - \mathbf{h}_i - \Delta\tau \tilde{Q}_i^{-1}\left(\mathcal{B}_i + \frac{W_i + W_{i+1}}{2}\right)\frac{\mathbf{h}_i + \mathbf{h}_{i+1}}{2}, \tag{B9}$$

and the measure of integration $\mathcal{D}\mathbf{h}$ as

$$\mathcal{D}\mathbf{h} = \prod_{i=0}^{N-1} \frac{d\mathbf{h}_{i+1}}{(2\pi\Gamma\Delta\tau)^{d/2}}. \tag{B10}$$

With the help of Eq. (B6), the transformation (B9) may be rewritten as

$$\boldsymbol{\psi}_{i+1} = \mathbf{h}_{i+1} - \mathbf{h}_i - \left(\frac{U_{i+1} - U_i}{2}\right)\left(\frac{U_i + U_{i+1}}{2}\right)^{-1}(\mathbf{h}_i + \mathbf{h}_{i+1}). \tag{B11}$$

This relation is easily inverted by setting $\mathbf{h}_i = U_i \boldsymbol{\zeta}_i$, which gives

$$\boldsymbol{\psi}_{i+1} = \left\{\frac{U_i + U_{i+1}}{2} - \frac{U_{i+1} - U_i}{2}\left(\frac{U_i + U_{i+1}}{2}\right)^{-1}\frac{U_{i+1} - U_i}{2}\right\}$$

$$\times (\boldsymbol{\zeta}_{i+1} - \boldsymbol{\zeta}_i)$$

$$= U_{i+1}\left(\frac{U_i + U_{i+1}}{2}\right)^{-1} U_i(\boldsymbol{\zeta}_{i+1} - \boldsymbol{\zeta}_i)$$

$$= \left(\frac{U_i^{-1} + U_{i+1}^{-1}}{2}\right)^{-1}(\boldsymbol{\zeta}_{i+1} - \boldsymbol{\zeta}_i),$$

so that we deduce (under the assumption $\mathbf{h}_0 = \mathbf{0}$), for $0 \leq i \leq N-1$,

$$\mathbf{h}_{i+1} = U_{i+1}\left[\sum_{j=0}^{i}\left(\frac{U_j^{-1} + U_{j+1}^{-1}}{2}\right)\boldsymbol{\psi}_{j+1}\right]. \tag{B12}$$

Since $\mathbf{h}_{i+1}$ is linearly related to the $\boldsymbol{\psi}_{j+1}$'s of index j lower than i, only the diagonal blocks $U_{i+1}[(U_i^{-1} + U_{i+1}^{-1})/2]$ enter the Jacobian of the transformation and one has

$$J_N \equiv \left|\frac{\partial \mathbf{h}_{i+1}}{\partial \boldsymbol{\psi}_{j+1}}\right| = \prod_{i=0}^{N-1} \frac{\det(U_i + U_{i+1})}{\det 2U_i}. \tag{B13}$$

To enforce the boundary condition $\mathbf{h}_N = \mathbf{h}_f$ at time τ_f in terms of the new variables $\boldsymbol{\psi}_i$, we introduce the usual integral representation of the δ function:

$$\delta^d(\mathbf{h}_f - \mathbf{h}_N) = \int \frac{d\boldsymbol{\alpha}}{(2\pi)^d} e^{-i\boldsymbol{\alpha}\cdot\{\mathbf{h}_f - U_N \sum_{i=0}^{N-1}[(U_i^{-1} + U_{i+1}^{-1})/2]\boldsymbol{\psi}_{i+1}\}}. \tag{B14}$$

After performing the Gaussian integration over the $\boldsymbol{\psi}_i$'s, one arrives at

$$Z[\mathbf{0} \to \mathbf{h}_f, \tau_f] = \prod_{i=0}^{N-1}\left\{\frac{\det(U_i + U_{i+1})}{\det 2U_i}\frac{1}{\sqrt{\det\tilde{Q}_i}}\right\}$$

$$\times e^{-(1/2\Gamma)\mathbf{h}_f \cdot W_N \mathbf{h}_f}$$

$$\times \int \frac{d\boldsymbol{\alpha}}{(2\pi)^d} e^{-i\boldsymbol{\alpha}\cdot\mathbf{h}_f} e^{-(\Delta\tau\Gamma/2)\boldsymbol{\alpha}\cdot G\boldsymbol{\alpha}}, \tag{B15}$$

where

$$G = U_N\left[\sum_{i=0}^{N-1}\left(\frac{U_i^{-1} + U_i^{-1}}{2}\right)\tilde{Q}_i^{-1}\left(\frac{{}^tU_i^{-1} + {}^tU_{i+1}^{-1}}{2}\right)\right]{}^tU_N. \tag{B16}$$

This awkward nonlocal operator G is greatly simplified when the singular initial condition already mentioned, $U_0 = \epsilon, W_0 = \epsilon^{-1}$ with $\epsilon \to 0^+$, is adopted. In that case, G is completely dominated by the first term of the series in the right-hand side of Eq. (B16) which diverges as ϵ^{-1} and, to leading order in ϵ, one has

$$G \approx \frac{1}{\Delta\tau} U_N(U_0^{-1} W_0^{-1t} U_0^{-1})^t U_N. \tag{B17}$$

The summation over $\boldsymbol{\alpha}$ can then be done and, since G^{-1} vanishes in the $\epsilon \to 0^+$ limit, one gets

$$Z[\mathbf{0} \to \mathbf{h}_f, \tau_f] = \left(\frac{1}{2\pi\Gamma\Delta\tau}\right)^{d/2}\frac{\det(U_0 + U_1)}{\det U_N}$$

$$\times \prod_{i=1}^{N-1}\left\{\frac{\det(U_i + U_{i+1})}{\det 2U_i}\frac{1}{\sqrt{\det\tilde{Q}_i}}\right\}$$

$$\times e^{-(1/2\Gamma)\mathbf{h}_f \cdot W_N \mathbf{h}_f}. \tag{B18}$$

Note that all the manipulations presented in this appendix were devoid of any approximation. It is finally a straightforward matter (details will be skipped here), to check that in the $\Delta\tau \to 0$ limit, the infinite product in front of the exponential in Eq. (B18) reduces to $(1/2\pi\Gamma\Delta\tau)^{d/2}(1/\sqrt{\det U_N})$, thereby making Eq. (B18) identical to the result (5.26) quoted in the text.

APPENDIX C

We consider the following quadratic action:

$$S_2[x_n] = \frac{1}{2}\sum_{n=0}^{d-1}\int_0^\tau d\tau \frac{\dot{x}_n^2}{a_n(\tau)}, \tag{C1}$$

where, in order to mimic the stochastic models studied in this paper, the variance $a_n(\tau)$ evolves on each shell as

$$a_n(\tau) = (\mathbf{b}^0 \cdot \mathbf{b}^0)(C_{n-2}^0 C_{n-1}^0)^2, \tag{C2}$$

i.e., as the variance of noise, $(\mathbf{b}^0 \cdot \mathbf{b}^0)B_{nn}$, for model (ii). In Eq. (C2), $\mathbf{b}^0(\tau)$ may be thought of as the deterministic self-similar solution, and $a_n(\tau)$ can therefore be cast into the form

$$a_n(\tau) = e^{2A_0\tau}\tilde{a}(\tau - nT_0), \qquad (C3)$$

where the function $\tilde{a}(\tau)$ satisfies

$$\tilde{a}(\tau + dT_0) = \tilde{a}(\tau) \qquad (C4)$$

because of the periodicity of the shell lattice. Let us assume that the instanton is centered around the shell of index $n = 0$ at time $\tau = 0$. At its leading edge $(n > 0)$, C_n decreases very abruptly as $\exp(-cr^n)$, with $r = (\sqrt{5} - 1)/2$ and c a constant of order 1. This essential singularity comes from the necessity of balancing $dC_n/d\tau$ with the dominant term $Q^2(1 - \epsilon)C_{n-2}C_{n-1}$ of the nonlinear kernel of the GOY model in this range of scales. In the trail of the instanton $(n < 0)$, one has a much smoother behavior $C_n \sim Q^{nz_0} \equiv e^{nA_0T_0}$. When the shell lattice is periodized, the leading edge and the tail of the instanton have to be glued together and the locus of matching, as well as the residual amplitude of C_n at that place, will be imposed by the side supporting the slowest variations of C_n. We conclude that in a cyclic chain containing d shells, most of them reside in the exponential tail of the instanton, so that we may write (again under the hypothesis of an instanton initially centered around the origin $n = 0$ and with a shell index n defined between 0 and $d - 1$)

$$a_n(0) \sim e^{4(n-d)A_0T_0}. \qquad (C5)$$

Thus, the range of values spanned by the function $\tilde{a}$ is very large and scales with the total number of shells like $e^{4dA_0T_0}$. For shells on the exponential ramp, $a_n(\tau)$ first decreases exponentially in time like $e^{-2A_0\tau}$ (because C_n decreases like $e^{-A_0\tau}$ in this region) and goes by a sharp maximum of order $e^{2nA_0T_0}$ at the time $\tau_n \sim nT_0$ when the center of the instanton reaches the corresponding shell. Then it starts again to decrease exponentially.

Having understood these basic dynamical features, we can compute the matrices U and W introduced in Sec. V A for the quadratic action given by Eq. (C1). To make contact with the normalized field $\mathbf{h}$ used in the real problem, we switch from the variable x_n to the variable $y_n = x_n/\sqrt{a_n}$. This transforms the original action into

$$S_2[y_n] = \frac{1}{2}\sum_{n=0}^{d-1}\int_0^\tau d\tau \left(\dot{y}_n + \frac{1}{2}\frac{\dot{a}_n}{a_n}y_n\right)^2. \qquad (C6)$$

Since there is no intershell coupling, the matrices U and W are diagonal in the shell index. The extremization of $S[y_n]$ with respect to y_n leads to the couple of first-order differential equations

$$p_n = \dot{y}_n + \frac{1}{2}\frac{\dot{a}_n}{a_n}y_n, \qquad (C7)$$

$$\dot{p}_n = \frac{1}{2}\frac{\dot{a}_n}{a_n}p_n. \qquad (C8)$$

One has simply $U_{nn} = y_n$ and $W_{nn}U_{nn} = p_n$. The solution of Eqs. (C7) and (C8) under the initial conditions $y_n(0) = 0$ and $p_n(0) = 1$ is

$$p_n(\tau) = \frac{\sqrt{a_n(\tau)}}{\sqrt{a_n(0)}}, \qquad (C9)$$

$$y_n(\tau) = \frac{1}{\sqrt{a_n(0)}}\frac{1}{\sqrt{a_n(\tau)}}\int_0^\tau a_n(\tau')d\tau'. \qquad (C10)$$

As long as $\tau < \tau_n = nT_0$, the instanton has not passed through the shell of index n and the integral in the right-hand side of Eq. (C10) is dominated by the neighborhood of the lower bound $\tau = 0$. We deduce that for indices $n > \tau/T_0$

$$U_{nn}(\tau) = \frac{e^{A_0\tau}}{2A_0}, \qquad (C11)$$

$$W_{nn}(\tau) = 2A_0e^{-2A_0\tau}. \qquad (C12)$$

By contrast, when τ gets larger than τ_n (by some units of time T_0), the integral on the right hand-side of Eq. (C10) is dominated by the neighborhood of the time τ_n where a_n takes its maximal value. We get

$$y_n(\tau) \sim I\sqrt{\frac{a_n(\tau_n)}{a_n(0)}}e^{A_0(\tau - \tau_n)},$$

$$p_n(\tau) \sim \sqrt{\frac{a_n(\tau_n)}{a_n(0)}}e^{-A_0(\tau - \tau_n)},$$

where I is a number of order 1. It follows that for indices $n < \tau/T_0$,

$$U_{nn}(\tau) \sim Ie^{2(d-n)A_0T_0}e^{A_0\tau}, \qquad (C13)$$

$$W_{nn}(\tau) \sim I^{-1}e^{2nA_0T_0}e^{-2A_0\tau}, \qquad (C14)$$

where we used the estimate (C5) for $a_n(0)$. Since $W_{nn}U_{nn} \sim e^{-A_0\tau}$ for $n > \tau/T_0$ and $\sim e^{2dA_0T_0}e^{-A_0\tau}$ for $n < \tau/T_0$, we conclude that $\det WU$ increases exponentially like $e^{dA_0\tau}$. But this property is not shared by $\det U$ or $\det W$ considered individually. Indeed, since the number of shells crossed by the instanton increases linearly in time, Eqs. (C11) and (C13) show that

$$\det U \sim \left(\frac{I}{2A_0}\right)^{\tau/T_0}e^{3A_0d\tau}e^{-A_0(\tau^2/T_0)}, \qquad (C15)$$

while from Eqs. (C12) and (C14),

$$\det W \sim \left(\frac{I}{2A_0}\right)^{-\tau/T_0}e^{-2A_0d\tau}e^{+A_0(\tau^2/T_0)}. \qquad (C16)$$

This argument captures apparently a good part of the physics of fluctuations around a moving self-similar system, though badly treating hybridization effects between neighboring shells. It also explains how large (small) numbers are generated in the spectrum of the matrix $U(W)$ and why in practice one does not have much freedom in the choice of the total number of shells d.

[1] E.D. Siggia, J. Fluid Mech. **107**, 375 (1981); Z.-S. She, E. Jackson, and S. Orszag, Proc. R. Soc. London, Ser. A **434**, 101 (1991); J. Jiménez, A. Wray, P.G. Saffman, and R. Rogallo, J. Fluid Mech. **255**, 65 (1993); F. Belin, J. Maurer, P. Tabeling, and H. Willaime, J. Phys. II **6**, 573 (1996).

[2] Reviewed by K. Gawedzki in *Advances in Turbulence VII*, edited by U. Frisch (Kluwer Academic, Dordrecht, 1998), pp. 493–502.

[3] For an introduction to shell models, see T. Bohr, M.H. Jensen, G. Paladin, and A. Vulpiani, *Dynamical Systems Approach to Turbulence and Extended Systems* (Cambridge University Press, Cambridge, 1998).

[4] E.D. Siggia, Phys. Rev. A **17**, 1166 (1978); T. Nakano, Prog. Theor. Phys. **79**, 569 (1988); G. Parisi (unpublished).

[5] J.-L. Gilson, and T. Dombre, Phys. Rev. Lett. **79**, 5002 (1997).

[6] See M.I. Freidlin and A.D. Wentzell, *Random Perturbations of Dynamical Systems* (Springer, New York, 1984) for the mathematical foundations of such computations.

[7] L.N. Lipatov, Zh. Éksp. Teor. Fiz. Pis'ma Red. **24** 179 (1976) [JETP Lett. **24**, 157 (1976)]; Zh. Éksp. Teor. Fiz. **71**, 2010 (1976) [Sov. Phys. JETP **44**, 1055 (1976)]; Pis'ma Red. Zh. Éksp. Teor. Fiz. **25**, 116 (1977) [JETP Lett. **25**, 104 (1997)]; Zh. Éksp. Teor. Fiz. **72**, 411 (1977) [Sov. Phys. JETP **45**, 216 (1977)].

[8] G. Falkovich, I. Kolokolov, V. Lebedev, and A. Migdal, Phys. Rev. E **54**, 4896 (1996).

[9] V. Gurarie and A. Migdal, Phys. Rev. E **54**, 4908 (1996).

[10] E. Balkovsky, G. Falkovich, I. Kolokolov, and V. Lebedev, Phys. Rev. Lett. **78**, 1452 (1997).

[11] M. Chertkov, Phys. Rev. E **55**, 2722 (1997).

[12] E. Balkovsky and V. Lebedev, Phys. Rev. E **58**, 5776 (1998).

[13] T. Dombre and J.-L. Gilson, Physica D **111**, 265 (1998).

[14] R. Benzi, L. Biferale, and G. Parisi, Physica D **65**, 352 (1993).

[15] U. Frisch, *Turbulence: The Legacy of A.N. Kolmogorov* (Cambridge University Press, Cambridge, 1995).

[16] C.W. Gardiner, *Handbook of Stochastic Methods for Physics, Chemistry, and the Natural Sciences*, Series in Synergetics (Springer-Verlag, Berlin, 1982), Vol. 13.

[17] P.C. Martin, E. Siggia, and H. Rose, Phys. Rev. A **8**, 423 (1973); C. de Dominicis, J. Phys. (France) **37**, 247 (1976); H. Janssen, Z. Phys. B **23**, 377 (1976).

[18] F. Langouche, D. Roekaerts, and E. Tirapegui, *Functional Integration and Semiclassical Expansions* (Reidel, Dordrecht 1982).

[19] I.M. Fomin and S.V. Guelfand, *Calculus of Variations* (Prentice-Hall, Englewood Cliffs, NJ, 1963).

[20] W. Dittrich and M. Reuter, *Classical and Quantum Dynamics*, 2nd ed. (Springer-Verlag, Berlin, 1994).

[21] Actually, this change of variable is not strictly necessary. It may be shown to roughly ''square root'' the range of values spanned by the coefficients of matrices U and W introduced in Sec. V A. The ensuing reduction of numerical stiffness allows computations at larger sizes of the shell lattice. However, the switch from $\delta\mathbf{b}$ to $\mathbf{h}$ gets totally impracticable when the matrix B cannot be easily inverted.

[22] L.S. Schulman, *Techniques and Applications of Path Integration* (Wiley, New York, 1981).

[23] L. Biferale, I. Daumont, T. Dombre, and A. Lanotte, Phys. Rev. E **60**, R6299 (1999).